DETERMINATION OF SURFACE AREAS OF FINELY DIVIDED MATERIALS BY THE PERMEABILITY METHOD

A THESIS

Presented to

the Faculty of the Graduate Division

by

Robert Allen McAllister

In Partial Fulfillment

of the Requirements for the Degree

Doctor of Philosophy

in the School of Chemical Engineering

Georgia Institute of Technology

June 1953

DETERMINATION OF SURFACE AREAS

OF FINELY DIVIDED MATERIALS BY

THE PERMEABILITY METHOD

Approved:

Date Approved by Chairman: May 29/1953

To

Ruth Heffner McAllister

PREFACE

I wish to pay tribute to my wife, Ruth Heffner McAllister, without whose faith, love, patience, and understanding this work would never have been completed. Her hard work and self denial alone made possible the time which was spent in this endeavor.

To Dr. J.M. DallaValle I owe much, both as a friend and as an advisor. His constant encouragment and excellent guidance have played a vital part in making this work worthwhile, if it is that. I am also indebted to Drs. F. Bellinger, R.F. Sessions, and K.M. Murphy for reading the text and making many suggestions.

ROBERT A. McALLISTER

Atlanta, Georgia

April, 1953

TABLE OF CONTENTS

TABLE OF CONTENTS (Concl.)

Page missing from thesis

LIST OF ILLUSTRATIONS

ABSTRACT

DETERMINATION OF SURFACE AREAS
OF FINELY DIVIDED MATERIALS BY
THE PERMEABILITY METHOD

(91 Pages)

by

Robert Allen McAllister

The determination of surface areas of finely divided materials by the permeability method involves the measurement of resistance to flow of a fluid through a bed of the fine particles. In a packed bed, the external surface of the particles provides the drag causing the pressure drop. Any cracks or fissures of near molecular size, or dead end capillaries as when there is a large interstitial area in the solid material, do not contribute to the shear stresses set up in the permeating fluid and hence do not contribute to the pressure drop. These "internal" surfaces then are not measured by the permeability method. Only the external surface can be so measured. The compactness of a given sample of solid material is another factor influencing the resistance to flow. Change of this factor alters the shape, size, and length of the flow passages within the bed which in turn affects the resistance of the bed to flow.

The permeability method of measuring surface areas has aroused

considerable interest since it is a relatively simple measurement to make. For those materials having little internal area, the measurement should give the total surface area, and for those powders having both internal and external area, this method should give the external area. To date, however, the accuracy of the method has been poor. Nevertheless, even though surface area is subject to uncertainty, the permeability method has proven to be of much value when employed as a comparative measure of fineness.

In deriving the relationship between the pressure drop, the surface area, and the bed structure, the bed is regarded as consisting of parallel capillaries of a single equivalent diameter. In the viscous flow region the pressure drop per unit length of the bed is then described by Poiseuille's law. The compactness of the bed is characterized by a porosity function . This function is defined as the ratio of the void volume to the total bed volume. An equation relating the surface area of particles to the permeability data was first derived by Carman (1), starting with Poiseuille's law to describe the flow.

The equation was found by Carman to be successful in determining the external surface area of comparatively large particles when a liquid was used as the permeating fluid. When much smaller particles are concerned and a gas is used as the permeating fluid, a correction must be made for molecular flow in the finer capillaries.

Molecular flow is a general flow regime where specular reflection of the molecules at the walls of the flow passage is not completely random. In other words, the velocity of the molecules at the wall

is not zero, as is required in the derivation of Poiseuille's law. The region of molecular flow begins where there is slip at the walls. This occurs when the pore or capillary diameter is still several times the mean free path of the gas molecules. When the mean free path is the same or larger than the pore diameter, the passage of the molecules in the pore is by diffusion and the flow is called Knudsen flow (2).

Lyon (3) has derived a permeability relation for gas flowing through porous media, including terms for both Poiseuille and Knudsen flow. The added correction for molecular flow in the Lyon equation improves the results of surface area calculations obtained from permeability data, but still the equation is not entirely satisfactory.

The purpose of this thesis is to reexamine the theory of the permeability method, using gas, and to attempt to improve the accuracy and reliability of the method.

The finely divided materials selected for testing were ones known to have little internal surface area. Five kaolin compounds, two emery grinding compounds, and one aluminum grinding compound were chosen having specific surface areas of from 0.3 to 12.3 square meters per gram. A weighed sample was placed in a cylindrical permeameter cell one inch in diameter. The bed was then compacted with a plunger fitted in the cell, by a single stroke, to either one hundred, three hundred, or five hundred pounds, depending on the porosity desired. Porosity values found with these powders were from 0.53 to 0.72. Three of the kaolin samples were tested at more than one porosity value, while the other samples were tested at a single porosity.

The cell containing the packed bed was connected in a manifold having a manometer to measure the pressure drop across the bed and a calibrated capillary tube with its manometer to measure the flow rate through the manifold. The flow rate was set by adjusting an air leak into a surge bottle installed downstream of the capillary and connected to a vacuum pump. Several settings of the flow rate were made for each sample, the range being limited by the amount of deflection available on the manometer measuring pressure drop across the bed (40 cm. red oil of 0.827 specific gravity).

Surface areas were calculated from these measurements on the basis of a modified Carman equation accounting for Poiseuillean flow (4), and by the Lyon equation, which adds a term accounting for free molecule flow. In addition a correlation was made on the basis of the Fanning friction factor-Reynolds number relation given in equation (1).

$$\frac{\Delta h g}{2u^2 L}\frac{4\epsilon}{(1-\epsilon)d_s S_w}\frac{1}{} = \phi\left\{\frac{4\epsilon^4}{(1-\epsilon)^3}\frac{u d}{\mu d_s}\ \frac{1}{S_w}\right\} \qquad (1)$$

The f vs, N_{Re} relation has become a standard in calculating the pressure drop, or the friction losses, in pipe, and equation (1) expresses it in terms of permeability data. A graph of the data was prepared in accordance with equation (1), the nitrogen adsorption surface area value for S_w being used for four of the samples. The value of S_w determined by nitrogen adsorption was used, since it is the best available measure of specific surface of finely divided materials. The line resulting from plotting the data on this basis was taken as the unique function described in equation (1). The equation of this unique

function was found to be

$$f = \frac{21.9}{N_{Re}} \quad . \tag{2}$$

Surface area values necessary to reduce the data of the other four samples to this unique function were then calculated. The results of all the considerations are these: 1. The surface area values calculated from the modified Carman equation accounting for Poiseuillean flow only, were lower than the nitrogen adsorption value by a factor of from 2.5 to 3.5. 2. The surface areas calculated from the Lyon equation were low also, but better than method 1, in general. 3. The surface area values calculated by using the f vs. N_{Re} method were both high and low, but the method gave the best values for the surface area using the permeability data.

S_w values as calculated from Carman's modified equation are consistently low. This indicates that the equation either does not describe the flow adequately, or that the flow is non-Poiseuillean. S_w values calculated from the Lyon equation are somewhat improved, but are still low. This indicates that a correction for molecular flow is necessary, but that the theory is still in need of improvement.

The calculation of surface area values by using the Fanning friction factor-Reynolds number relation provides the most accurate value derived from the permeability data. Other data given in the literature are insufficient for application to the Fanning friction factor-Reynolds number relation.

It is recommended that more data be obtained extending the

limits of the f vs. N_{Re} relation, including a wider range of porosity. Thus the applicability of the method can be further verified and extended.

The data indicate that at very low flow rates (about one cubic centimeter per hour), there is an added resistance to flow, not accounted for by any of the theoretical equations mentioned above. The explanation is offered that at very low shear stresses in the fluid (gas), the viscosity is no longer constant, but that it increases. If such a phenomenon exists, it clearly warrants further investigation.

Nomenclature

d	the gas density, grams per cubic centimeter
d_s	the solid density of the material composing the bed, grams per cubic centimeter
f	the Fanning friction factor equal to $\frac{\Delta h g 4 \epsilon}{2u^2 L(1-\epsilon)d_s} \frac{1}{S_w}$, dimensionless
g	the acceleration of gravity, centimeters per second per second
Δh	the static or pressure head equal to $-\Delta P/gd$, centimeters
L	the length of the bed, centimeters
ΔP	the pressure drop across the bed, dynes per square centimeters
S_w	the specific surface of the solid, square centimeters per gram
u	the superficial velocity, the velocity of the gas as if it were flowing through an empty permeameter cell, centimeters per sec.
ϵ	the porosity, void volume divided by the total volume
μ	the viscosity of the gas, poise
ϕ	any function of the argument

Literature Cited

(1) Carman, P.C. Trans. Inst. Chem. Engrs. , London, 15(1937) p.150.

(2) Knudsen, M. Ann. Physik. , 28(1909) p.75.

(3) Lyon, L.L. and Others. The Permeability Method of Determining Surface Areas of Finely Divided Materials. Wichita: University of Wichita Foundation, 1951.

(4) Lea, F.M. and Nurse, R.W. Symposium on Particle Size Analysis, London: Inst. of Chem. Engrs., 1947. p.48.

Approved: _____
Thesis Advisor

Date: May 29, 1953

CHAPTER I

INTRODUCTION

The determination of surface areas of finely divided materials by the permeability method involves the measurement of resistance to flow of a fluid through a bed of the fine particles. The resistance is formulated as the pressure drop per unit length of bed, and is a function of the external surface area of the material, the tortuosity of the flow, the compaction of the bed, and the properties of the permeating fluid. Since the pressure drop and the resistance to flow depend on the interaction of the fluid with a solid surface, only that portion of the particles actually exposed to flow can be related to the pressure drop. That is, if the material contains cracks or fissures of near molecular size, or if it contains "ink-bottle" or dead end capillaries, or a large interstitial surface area, then these latter surfaces will be dead spaces insofar as their contribution to the shearing forces causing pressure drop is concerned.

The permeability method of measuring surface areas has aroused considerable interest, principally because of the simplicity of the apparatus and its ease of operation when air is used as the permeating fluid (1), (2), (3), (4). Carman's original work (5), (6), (7) in developing the Kozeny equation showed that the permeability method, using a liquid as the permeating fluid, gave accurate results for comparatively coarse materials of varying shapes. Recent work on finer

powders, however, shows that the simple theory requires some modification (8). In particular, with a liquid as the permeating fluid, some workers consider that a correction must be applied for the amount of liquid adsorbed on the solid surface, and with gases correction must be made for molecular flow in the finer capillaries (9).

Molecular flow is a general flow regime where specular reflection of the molecules at the walls of the flow passage is not completely random. That is to say, the velocity of the molecules at the wall is not zero, as is required in the derivation of the Kozeny equation and Poiseuille's law. The region of molecular flow is begun where there is slip at the walls. This occurs when the pore or capillary diameter is still several times the mean free path of the molecules. When the mean free path is the same or larger than the pore diameter, the passage of the molecules in the pore is by diffusion and the flow is called Knudsen flow (10), (11), (12), (13).

In spite of the corrections applied, the theoretical formulas to date have been unable to define the surface areas of fine powders in terms of gas, or air, permeability data. Nevertheless, even though the absolute figure for specific surface is subject to uncertainty, the permeability method has proven to be of much use when employed as a comparative measure of fineness. Both the Bureau of Standards and the British Standards Institution have adopted the method in defining the fineness of cement (14), (15). For comparative fineness determinations, the accuracy of the surface area, or whether external or internal surface is involved is not so important as consistency from one batch to the next. The permeability measurement, being simple to make, is quite

suitable for such a control procedure.

Many materials, such as fillers, some powdered metals, grinding powders, and sands, are known to have very little internal surface area. In some of the catalytic operations, and in filtering operations, it is desirable to know the external area in addition to the total surface area. For these applications the permeability method should be capable of supplying reliable information concerning the external surface area.

It was the purpose of the study undertaken in this thesis to measure the permeability of several materials to air, and to apply the results to the three equations derived below: the Iea and Nurse equation, equation (14); the Lyon equation, equation (36); and the Fanning friction factor-Reynolds number relation, equation (48). In this manner it can be decided which derivation describes the flow variables the best, and which method gives the best results for a surface area value.

The surface area value derived from the permeability data will be compared with the nitrogen adsorption value, which value will be assumed to be the correct one for the material. The powders tested will be ones whose surfaces are known to be largely, if not entirely external.

An additional correlation will be presented, based on the Fanning friction factor-Reynolds number relation, which allows a more accurate calculation of the surface area from permeability data.

CHAPTER II

THEORY

The Lea and Nurse Equation

The extension of Carman's work (5),(6),(7) on the viscous flow of liquids through porous media to include measurements with gases was first made by Lea and Nurse (16). A portion of Carman's derivation, along with the entire Lea and Nurse derivation, is presented to show the theory involved.

Streamline Viscous Flow of an Incompressible Fluid.--In the general study of fluid flow through non-circular channels, the "mean hydraulic radius" must be utilized instead of the radius in order that the theory for circular channels can be extended to other shapes. The hydraulic radius is defined as:

$$m = \frac{\text{cross sectional area normal to flow}}{\text{perimeter presented to fluid}} , \qquad (1)$$

and for a uniform bore is equivalent to

$$m = \frac{\text{volume of fluid in pipe}}{\text{surface presented to fluid}} . \qquad (2)$$

For a circular pipe $m = D/4$. In his derivation of the Kozeny equation, Carman assumes that a bed formed from a granular material is equivalent to a group of similar parallel channels. Therefore the total internal surface of the pore channels is equal to the total external surface of the powder, and the total internal volume of the channels is equal to the pore space in the powder bed. If ϵ is the porosity, then in one

cc of the bed the channel volume will be ϵ and the channel surface will be $S_v(1-\epsilon)$ where S_v is the specific surface in square centimeters of solid volume. Converting to sq. cm. per gm. (S_w) requires that $S_v = d_s S_w$ where d_s is the density of the powder. The hydraulic radius is then

$$m = \frac{\epsilon}{d_s S_w (1 - \epsilon)} , \tag{3}$$

Poiseuille's Law for a circular channel is as follows:

$$u = \frac{D^2 \Delta P}{32 \mu L} = \left(\frac{D}{4}\right)^2 \frac{\Delta P}{2 \mu L} . \tag{4a}$$

By remembering that for a circular pipe $m = D/4$, it is seen that for a channel of non-circular cross section,

$$u_c = \frac{m^2 \Delta P}{k_o \mu L_c} \tag{4b}$$

where

u_c = velocity of the fluid in the channel, or capillary, cm./sec.,

ΔP = pressure drop across the bed, dynes/cm.^{2},

k_o = a factor depending on the shape of the channel,

μ = viscosity of the fluid, poise, and

L_c = the length of path traversed by the fluid.

In any actual experiment on a cylindrical bed of powder, the velocity is calculated on the basis of the area of the empty container, and may be called the superficial velocity, u. If the pores are all parallel and of equal diameter, then the velocity in the pores, u_d, is greater than the superficial velocity by the factor $1/\epsilon$. If the pores are not parallel, but circuitous, then the pore velocity is greater

then in the parallel capillary case by the factor L_c/L, where L is the over-all length of the bed.

Therefore,

$$u = u_c \epsilon \frac{L}{L_c} . \tag{5}$$

Substitution of equation (4b) into equation (5) gives

$$u = \frac{\epsilon}{k_o}\left(\frac{L}{L_c}\right)^2 \cdot \frac{m^2 \Delta P}{\mu L} , \tag{6}$$

and inserting the value of m from equation (3) gives

$$u = \frac{\epsilon^3}{(1-\epsilon)^2} \cdot \frac{1}{k_c}\left(\frac{L}{L_c}\right)^2 \cdot \frac{1}{S_w^2 d_s^2} \frac{\Delta P}{\mu L} , \tag{7}$$

or

$$u = \frac{\epsilon^3}{(1-\epsilon)^2} \cdot \frac{\Delta P}{k \mu L S_w^2 d_s^2} , \tag{8}$$

where k is known as Kozeny's or Carman's constant

This derivation of the Kozeny equation follows closely that given by Carman, but is reproduced here in order to draw attention to the nature of the constant k. Since

$$k = k_o \frac{L_c^2}{L} , \tag{9}$$

it cannot be constant for any given channels taken separately, but may be essentially constant when the actual measured flow is the sum of that from numerous interconnected channels as in a powder bed. There has been considerable discussion concerning the constant k. Sullivan and Hertel (17) have described this constant as:

$$k = \frac{k_o}{k_1} = 5.0 \text{ for most cases.} \qquad (10)$$

They consider k as a dimensionless quantity, called a shape factor, which depends upon the shape of the conduit through which viscous flow is taking place. The factor k_o has a value of 2.0 for circular conduits, as seen by comparing equations (4a) and (4b), while for irregularly shaped conduits for value may be as high as 3.0. They also consider k_1 as an orientation factor which accounts for the influence of the orientation of the individual particles composing the medium upon flow. Sullivan and Hertel estimate, from theoretical considerations that the factor k_1 is equal to 1.0, 0.67, and 0.5 for the cases of viscous flow parallel to cylinders, flow through a bed of spheres, and flow perpendicular to cylinders, respectively. Regardless of such attempts to attach physical significance to the k constant, Carman (6) has shown that a value for k of 5.0 is substantially correct for liquid flow through porous media.

The Determination of Surface Area.--The experimental apparatus used by Lea and Nurse in their measurements of gas permeability was similar to that used by the author (see Figure 1). Their flowmeter was a capillary tube, calibrated so that the deflection of a manometer was related to the flow rate by the following equation:

$$Q = \frac{C\, h_2\, d_m}{\mu} \qquad (11)$$

where Q = the flow rate, $cm.^3/sec.$,

C = a constant for a given capillary, $cm.^4/sec.^2$,

h_2 = difference in level of liquid in manometer measuring pressure difference across the capillary, cm., and

d_m = density of the liquid in the manometer, gm./cm.^{3}

From equations (8) and (11):

$$Q = uA = \frac{\epsilon^3}{(1-\epsilon)^2} \cdot \frac{\Delta PA}{k \mu L S_w^2 d_s^2} = \frac{Ch_2 d_m}{\mu} \qquad (12)$$

The pressure drop is measured on another manometer, which also contains a liquid of density d_m. Hence $\Delta P = h_1 d_m g$, where g is the acceleration of gravity in cm./sec.^{2}, and therefore,

$$S_w = \frac{\sqrt{g/k}}{d_s(1-\epsilon)} \sqrt{\frac{\epsilon^3 A h_1}{C L h_2}} \cdot \qquad (13)$$

Taking Carman's value of 5.0 for k,

$$S_w = \frac{14}{d_s(1-\epsilon)} \sqrt{\frac{\epsilon^3 A h_1}{C L h_2}} \cdot \qquad (14)$$

Equation (14) is the Lea and Nurse equation for calculating the surface area of finely divided materials. Once the orifice calibration has been made, the determination of a surface area value with the use of this equation is very simple, requiring but a single flow rate setting. The surface areas calculated by this method are consistently low (compared to the nitrogen adsorption surface areas), and objections have been raised concerning the validity of the equation at high pressure differential values. These objections will be included in the derivation of the Lyon equation below.

The Lyon Equation

Lyon (18) has presented a comprehensive theory of the flow of a compressible gas through a porous medium. He considers a system where

gas is flowing through a porous bed from a high pressure side P_1 to a low pressure side P_2. The flow of a compressible gas through such a medium can be described in terms of at least two limiting types of flow. If the dimensions of the voids in the porous medium are considerably larger than the mean free path of the gas, the flow will be of the viscous type. For pressures ordinarily utilized in permeability measurements (near atmospheric and below) and with finely divided powders, the resistances to flow are so high that the turbulent flow region is never entered. Undoubtedly if the upstream pressure were increased sufficiently, for a given downstream pressure, turbulent flow could be attained. Turbulence may cause shifting of the particles in the bed, making a steady state condition impossible. Turbulent flow may have been avoided purposely, since theoretical treatment of the hydrodynamics in the region is not entirely satisfactory. As the mean free path is lengthened for a given pore diameter, or as the pore diameter is made smaller the gas no longer adheres to the walls in accordance with Poiseuille's equation. In the viscous region where the flow follows Poiseuille's law, the pore or capillary diameter is much larger than the mean free path in the gas. At a given cross section there are many more collisions between the gas molecules themselves than there are between the gas molecules and the walls of the passage. Thus the momentum transfer between successive differential annuli results in the familiar parabolic velocity gradient across the capillary, with a zero velocity at the wall. Another way of visualizing a zero velocity at the wall is to assume that there are sufficient collisions of the slowly moving gas molecules a mean free path removed from the wall and that the rebounds from these collisions strike

the wall in random directions, completely independent of the bulk flow of gas through the capillary. Where the mean free path of the gas molecule is longer than the pore diameter, viscosity is no longer a factor since the number of collisions of the gas molecules with the walls is many times the number of collisions between the gas molecules themselves. This flow condition is essentially gas diffusion through a tube. This type of flow is termed Knudsen or free molecule flow (10), (11), and (13).

Between these two extremes is a region where the flowing gas slips along the wall. A gas molecule strikes the wall about (a very broad interpretation of "about" is intended here) as many times as it does another gas molecule. As a result no well-defined velocity gradient terminating with a zero velocity at the wall can be established. In other words, there are not enough collisions in the gas, compared with those with the wall, to provide the viscous drag necessary for a zero velocity at the wall. For this intermediate region between Knudsen and Poiseuillean flow, Present and deBethune (19) as well as Arnell (20), (21) affirm that for pure gases the free molecule flow and viscous flow components are strictly additive.

In this discussion the flow characteristics of a porous medium will be described in terms of its conductance, F. Fluid conductance corresponds to the rate of flow per unit difference of pressure. The flow is expressed in pressure-volume terms. The conductance of a gas through a porous medium can be described by the equation

$$F = \frac{K_1}{S_v^2} \cdot \bar{P} + \frac{K_2}{S_v} , \qquad (15)$$

where $\bar{P}$ = the average pressure of the gas in the bed $\frac{P_1 + P_2}{2}$,

K_1 = a constant pertaining to viscous flow, and

K_2 = a constant pertaining to free molecule flow.

The first term of equation (15) expresses the amount of conductance that can be described from a consideration of viscous flow. Similarly, the second term expresses the amount of conductance that can be described from a consideration of Knudsen flow. According to this equation, if the total conductance F is plotted against the average pressure $\bar{P}$, a straight line should result. If free molecule flow alone is occurring the slope of the line would be zero, while if only viscous flow occurs, the line would have a finite slope and pass through the origin. For the intermediate case the line would have a finite slope and a definite intercept value. The evaluation of the functions K_1 and K_2 is now presented.

Viscous Flow of a Compressible Fluid through a Porous Medium.--The following equation was proposed by Carman (5) for the flow of liquids through a porous medium:

$$Q = \frac{\Delta P A}{\mu S_v^2 k L} \cdot \frac{\epsilon^3}{(1-\epsilon)^2} \cdot \qquad (16)$$

This equation is identical with equation (12). Carman in his derivation of equation (16) started from a consideration of the familiar Poiseuille equation, (4a), involving the flow of a liquid through a capillary tube of radius r.

$$Q = uA = \left(\frac{4r^2 \Delta P}{32 \mu L}\right) \cdot \left(\pi r^2\right) = \frac{\pi r^2 \Delta P}{8 \mu L} \cdot \qquad (17)$$

The Poiseuille equation assumes the following form for the viscous flow of a gas through a capillary (22):

$$PQ = \frac{\pi r^4}{8 \mu L} \cdot \frac{(P_1^2 - P_2^2)}{2} \cdot \tag{18}$$

If the volume of gas flowing through the capillary is measured at pressure P_1, then,

$$Q = \frac{\pi r^4 \Delta P}{8 \mu L} \cdot \frac{\overline{P}}{P_1} \cdot \tag{19}$$

Starting with equation (19) and following the derivation used by Carman for liquids, the equation describing the viscous flow of gases through porous media would be

$$Q = \frac{\Delta P A}{\mu S_v^2 k L} \cdot \frac{\epsilon^3}{(1-\epsilon)^2} \cdot \frac{\overline{P}}{P_1} \cdot \tag{20}$$

Since most of the investigations involving viscous flow of gases through porous media have been conducted at very low differential pressures, the value of $\overline{P}/P_1$ was essentially one, and thus the use of equation (15) in place of (20) did not affect the results appreciably. However, in those investigations using large differential pressures, the use of equation (15) would be of little value.

If the volume of gas flow per second is measured at P_1 the conductance would be defined as

$$F = Q P_1 / \Delta P .$$

The value of K_1 in equation (15) is therefore

$$K_1 = \frac{A}{\mu kL} \cdot \frac{\epsilon^3}{(1-\epsilon)^2} \cdot \qquad (21)$$

Free Molecule Flow of a Gas through a Porous Medium.--In this type of flow, the mean free path of the gas is so large, compared to the dimensions of the voids in the medium, that the only collisions experienced by the gas molecules are those with the surface of the medium. This situation can be considered as being the same as low pressure gas diffusion, usually called Knudsen or free molecule flow.

Let F equal the average number of molecules crossing in unit time a unit of area perpendicular to direction x, the direction of flow, or the direction of the pressure drop. Then from the generalized definition of the diffusion coefficient D,

$$F = -D \frac{dn}{dx} \quad , \qquad (22)$$

where D = diffusion coefficient, and

$\frac{dn}{dx}$ = rate of change of the number of molecules per unit volume in direction x.

According to discussions in Pollard and Present (23), the Knudsen diffusion of a gas in an irregular capillary or in a porous medium is very similar to diffusion in a tube of infinite length. They also present an argument used by Bosanquet (24) that the diffusion coefficient for a gas, in which the successive steps of individual molecules are terminated by wall collisions, is $D=2\bar{v}r/3$, where r is the radius of the tube and $\bar{v}$ is the mean molecular speed.

It is assumed, therefore, that the value of D in the case of a gas undergoing free molecular flow through a porous medium is

$$D = 2\bar{v}r/3 \quad , \tag{23}$$

where r = the average pore radius of the pores in the porous medium.

The transport, or the number of molecules of gas flowing through one pore of a porous medium, would be

$$\bar{\Gamma} = -2\bar{v}r/3 \frac{dn}{dx} \quad . \tag{24}$$

Consider a system where gas is flowing through a porous medium at constant temperature from a high pressure side P_1 to a low pressure side P_2. The number of molecules per unit volume on the high pressure side is $n_1 = P_1/kT$, and the corresponding value $n_2 = P_2/kT$ for the low pressure side. The k referred to here is the Boltzmann constant and not to be confused with the Carman or Kozeny constant.

In the case where the mean free path is much larger than the dimensions of the pores, all portions of the system are effective in determining the transport. Since, in a porous medium, a portion of the system that would ordinarily effect transport is occupied by solids, the effective number of molecules per unit volume contributing to transport is proportional to ϵ, the porosity of the medium. It is assumed that the number of molecules per unit volume that contribute to transport varies from $n_1\epsilon$ to $n_2\epsilon$. Therefore,

$$-\frac{dn}{dx} = \frac{\epsilon(P_1-P_2)}{kTL} \quad , \tag{25}$$

where L = the length of the porous medium

k = Boltzmann constant in this case.

The minus sign arises from a negative pressure gradient. It should be stressed that k represents the Boltzmann constant only in equations (25), (26), (27), and as noted above. In all other cases it represents the Carman constant.

With these considerations equation (24) becomes

$$\bar{F} = 2\bar{v}r/3 \cdot \frac{\epsilon (P_1-P_2)}{kTL} \tag{26}$$

From kinetic theory we have the relations

$$kT = \frac{\pi m\bar{v}^2}{8} \text{ , or } \bar{v} = 2\sqrt{\frac{2RT}{\pi M}} \text{ ,} \tag{27}$$

where m = mass of one molecule,

R = gas constant per mole, and

M = molecular weight of the gas

Substitution of the relations in (27) into equation (26) result in

$$\bar{F} = \frac{\epsilon (P_1-P_2)}{mL} \cdot \frac{8r}{3\pi\sqrt{\frac{2RT}{\pi M}}} \tag{28}$$

The grams of gas transported per unit area of pore by one pore will be $m\bar{F}$. Hence, the total grams, G, transported by N pores of individual cross sectional area πr^2 must be

$$G = N\pi r^2 m \bar{F} \text{ ,}$$

or

$$G = \frac{\epsilon (P_1-P_2)}{L} \cdot \frac{8r^3N}{3\sqrt{\frac{2RT}{\pi M}}} \text{ .} \tag{29}$$

Since it was assumed that there are N pores of radius r, the definition of porosity provides the relation that

$$\epsilon = \frac{N \pi r}{A} \tag{30}$$

The surface area S_v of the porous material per unit volume of solid is

$$S_v = \frac{2N\pi r^2}{A(1-\epsilon)} \cdot \tag{31}$$

If equation (31) is solved for r and equation (30) for N, the following relation may be derived:

$$N \pi r^3 = \frac{2A\epsilon^2}{S_v(1-\epsilon)} \cdot \tag{32}$$

In pressure-volume terms G is PQM/RT where Q is the volume rate of flow. Using this relation along with equation (32) and substituting into equation (29), the following is derived:

$$PQ = \frac{\epsilon^3 (P_1-P_2)}{L} \cdot \frac{8A}{3S_v(1-\epsilon)} \cdot \sqrt{\frac{2RT}{\pi M}} \cdot \tag{33}$$

If the volume rate of flow is measured at pressure P_1, then the left side of equation (33) is P_1Q.

Thus, K_2 of equation (15) has been derived as:

$$K_2 = \frac{8}{3}\sqrt{\frac{2RT}{\pi M}} \cdot \frac{A}{L} \cdot \frac{\epsilon^3}{(1-\epsilon)} \cdot \tag{34}$$

By substituting the value of K_1 from equation (21) and the value of K_2 from equation (34), equation (15) can be written

$$F = \frac{QP_1}{\Delta \bar{P}} = \frac{A\epsilon^3}{\mu k l S_v^2 (1-\epsilon)^2} \cdot \bar{P} + \frac{8}{3}\sqrt{\frac{2RT}{\pi M}} \cdot \frac{A}{lS_v} \cdot \frac{\epsilon^3}{(1-\epsilon)} , \tag{35}$$

or, in terms of S_w,

$$F = \frac{QP_1}{\Delta P} = \frac{A\epsilon^3}{kLS_w^2 d_s^2 (1-\epsilon)^2} \cdot \overline{P} + \frac{8}{3}\sqrt{\frac{2RT}{\pi M}} \cdot \frac{A}{LS_w d_s} \cdot \frac{\epsilon^3}{(1-\epsilon)} \cdot \qquad (36)$$

Equations (35) and (36) describe the flow of a gas through a porous medium, according to the Lyon derivation.

Fanning Friction Factor - Reynolds Number Correlation

A convenient method of deriving the relationship between the Fanning friction factor and the Reynolds number is by the use of dimensional analysis. Consider the pressure drop due to friction for isothermal flow at a constant mass rate through a packed bed. If the flow is assumed to be streamlined, then experimental data shows the density does not enter as a factor (25). It is then assumed that the quantities which control the flow are L, D_c, u_c, μ, ϵ, and a shape factor. The last two factors are dimensionless and hence will be ignored for the moment.

If

$$-\frac{\Delta P}{L} = \phi\,(D_c, u_c, \mu), \qquad (37)$$

it may be replaced by an infinite series,

$$-\frac{\Delta P}{L} = K D_c^{a} u_c^{b} \mu^{c} = K' D_c^{a'} u_c^{b'} \mu^{c'} + \ldots \qquad (38)$$

In equation (38), the dimensionless factor K, and the dimensionless exponents may have any value to describe the situation. All of the terms of the series are of the same form, and therefore attention may be focused only on the first term. Substitution is now made of the dimensions of the factors in the MLθ system in accordance with the notation given in reference (25):

$$(M\,L^{-2}\theta^{-2}) = (L^{a})\,(L^{b}\,\theta^{-b})\,(M^{c}\,L^{-c}\,\theta^{-c}$$

Σ M: $\quad 1 = c \qquad \therefore\ c = 1$

Σ L: $\quad -2 = a+b-c \qquad \therefore\ a = -2$

$\Sigma\,\theta$: $\quad -3 = -b-c \qquad \therefore\ b = 1$.

Therefore:

$$-\frac{\Delta P}{L} = K\frac{u_c \mu}{D_c^{\,2}} \ . \tag{39}$$

It is desirable to derive an expression for the mean pore diameter D_c, in terms of the porosity function. By recalling equation (1), it is remembered that:

$$m = \text{hydraulic radius} = \frac{\text{cross-sectional area normal to flow}}{\text{perimeter presented to the fluid}} \ . \tag{1}$$

Assuming circular pores of uniform diameter throughout the bed,

$$m = \frac{D_c}{4} = \frac{\text{area for flow}}{\text{wetted perimeter}} \times \frac{L}{L} = \frac{\text{void volume}}{\text{total surface}} = \frac{V_v}{S_t} \ . \tag{40}$$

The ratio of the void volume, V_v, to the total volume, V_t, is the porosity, ϵ . Therefore, since

void volume + solid volume = total volume,

$$V_v + V_s = V_t \ , \text{ and} \tag{41}$$

by dividing equation (41) by V_v and substituting the definition of porosity, it can be derived that:

$$V_v = \frac{\epsilon}{1-\epsilon} V_s \ . \tag{42}$$

Substitution of this value of V_v into equation (40) gives

$$D_c = \frac{4\epsilon}{(1-\epsilon)S_v} \quad . \tag{43}$$

Combination of equations (43) and (39) results in

$$-\frac{\Delta P}{L} = K \frac{u_c \mu (1-\epsilon)^2 S_v^2}{16 \epsilon^2} \quad . \tag{44}$$

If it is assumed that $u_c = u/\epsilon$ and $S_v = 6/D_c$, then,

$$-\frac{\Delta P}{L} = K \frac{u \mu 36}{D_c^2 16} \cdot \frac{(1-\epsilon)^2}{\epsilon^3} \quad . \tag{45}$$

It is noted that equation (45) is equivalent to equation (7) above. If equation (45) is multiplied by $D_c/2u^2 d$,

$$-\frac{\Delta P}{d} \cdot \frac{D_c}{2u^2 L} = K' \frac{\mu}{D_c u d} \cdot \frac{(1-\epsilon)^2}{\epsilon^3} \tag{46}$$

The left-hand side of equation is termed the Fanning friction factor, f, and the right side of the equation is a function corresponding to the Reynolds number, N_{Re}.

The pressure drop may be expressed in terms of height of fluid flowing, Δh, as:

$$-\frac{\Delta P}{d} = \Delta h \, g \quad , \tag{47}$$

where g is the acceleration of gravity. Thus,

$$\frac{\Delta h \, g \, D_c}{2u^2 L} = f = \phi \left[\frac{D_c u d}{\mu} \cdot \frac{\epsilon^3}{(1-\epsilon)^2} \right] = \phi N_{Re} \quad . \tag{48}$$

Equation (48) expresses a relationship among the variables when a fluid is flowing through a porous medium.

CHAPTER III

EQUIPMENT

The equipment used to determine the permeability of packed beds of finely divided materials is shown in Figure 1. The powder being measured was packed into the permeameter cell and placed in the system as shown. Dry air was drawn through the bed by means of a vacuum pump connected downstream. Manometers Nos. 1 and 2 (see Figure 1) contained red manometer oil and indicated the pressure drop across the permeameter cell and capillary orifice respectively. Manometer No. 3 was used as a check in measuring the pressure downstream of the orifice. One side was open to atmospheric pressure and the other side was connected to the surge bottle. Either water or mercury was the fluid used in manometer No. 3, depending on the magnitude of the pressure differential. A surge bottle, having a capacity of 24 liters, was inserted upstream of the vacuum pump to minimize the effect of any pressure fluctuations. This bottle was supplied with a connection to the atmosphere which could be adjusted so as to give a controlled leak into the surge volume. This allowed the pressure in the bottle, and hence the flow rate through the bed, to be set at a given value.

The manometer levels were measured with a 100-cm. cathetometer capable of providing readings to a tenth of a millimeter. In addition to insuring that the cathetometer bar was vertical -- done by centering a bubble on the base of the instrument -- it was necessary to have the

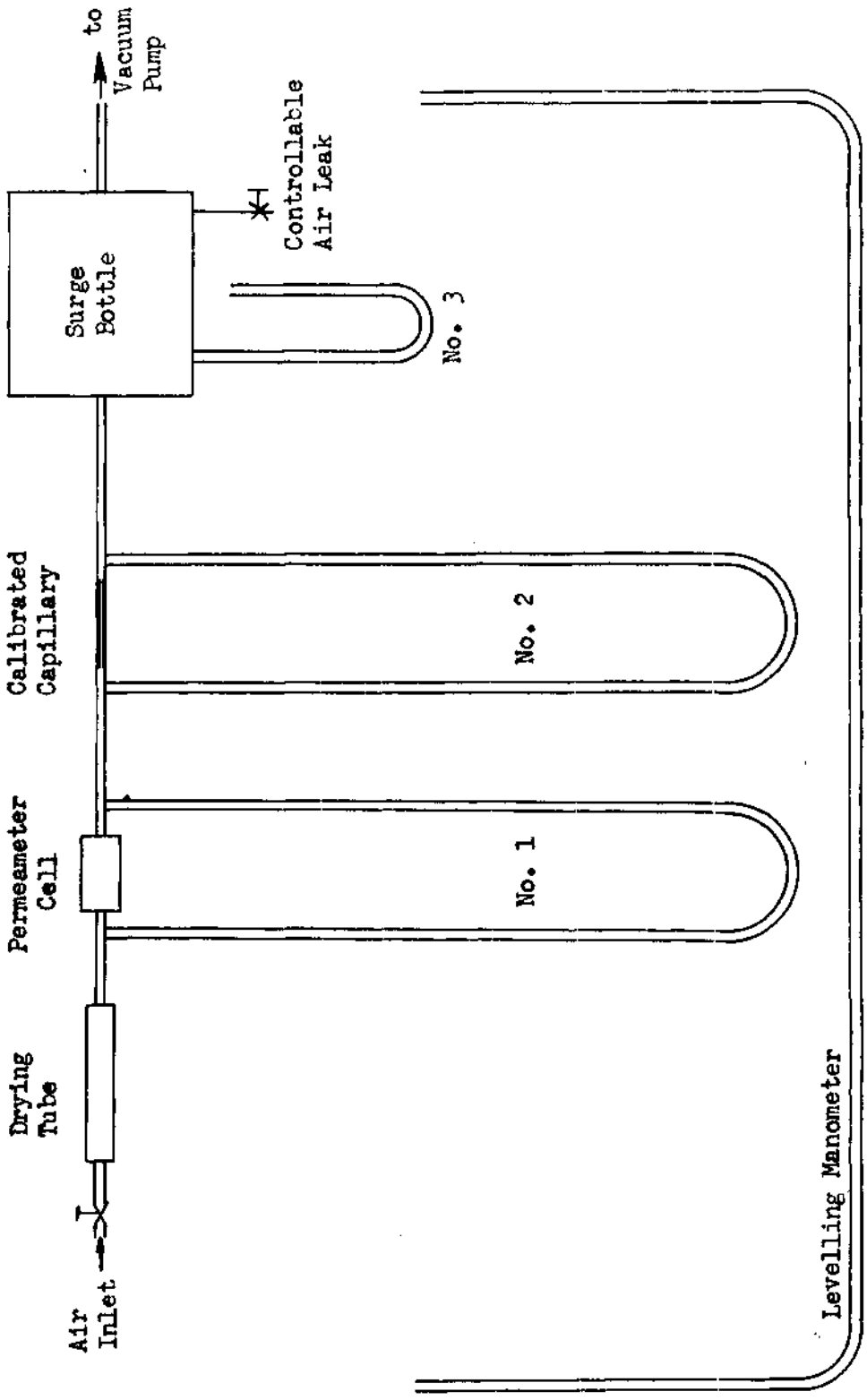

Figure 1. Permeameter Assembly

sighting telescope perfectly level. This was done by adjusting the telescope until no difference in height could be detected on the meniscii of the levelling manometer shown in Figure 1.

The permeameter cell assembly is shown in Figure 2. The powder sample being tested was placed in the cylindrical cavity and packed with the plunger. After the powder was packed, and before the plunger was removed from contact with the sample, the indicator nut was screwed down until it touched the top of the cylinder, and the lock nut was jammed against it. When the plunger was removed, the depth that it had been inserted was measured between the end and the indicator nut with a depth gage. This measurement, along with the depth of the empty cylinder, was used to calculate the bed depth.

The plunger and its attendant nuts were not used with the cell while measurements on the air flow were being made in the permeameter assembly. The fine particles comprising the bed rested on a piece of filter paper fitted on top of the perforated plate between the cylinder and the plate. The plate was 1/16 inches thick with sixty-four 1/16-inch diameter holes drilled in it.

The entire permeameter cell was made of brass. The bed cavity was 1.000 inches in diameter and two inches long.

The components of the permeameter assembly were connected with rubber tubing. Three sizes of capillaries were used with manometer No. 2 in measuring the flow rate. The smallest was made from a broken thermometer containing a very fine hole. The largest capillary was one millimeter in diameter. An intermediate orifice was made by drawing down a one-millimeter capillary. The capillaries were approximately

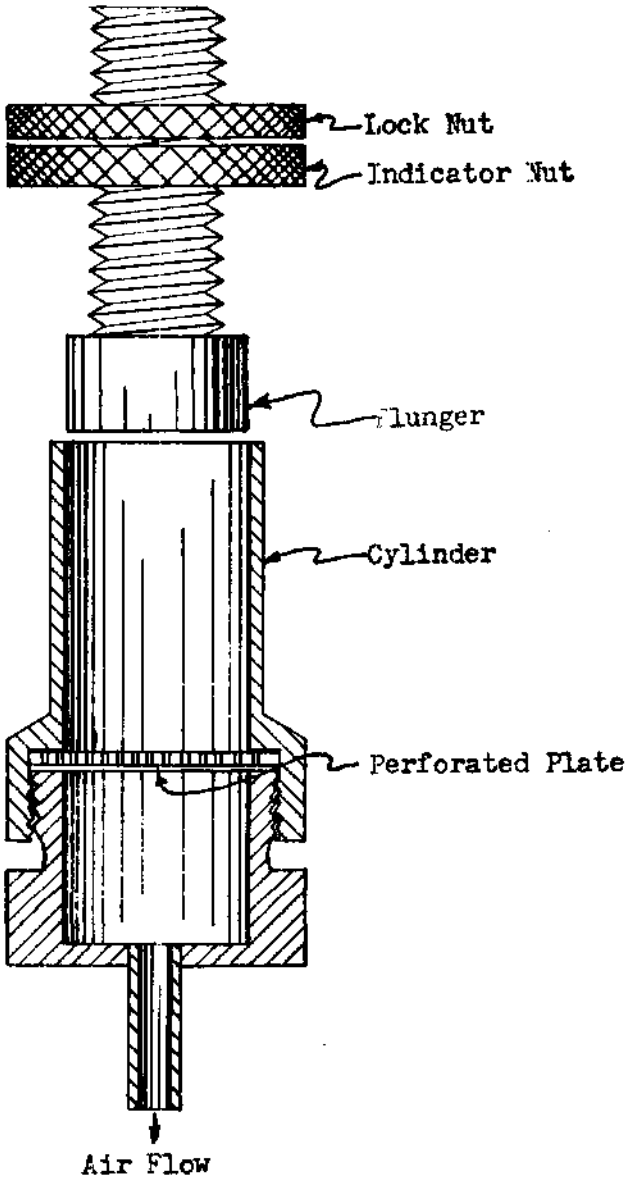

Figure 2. Permeameter Cell Assembly

four inches long. No measurement was made of the exact size of the capillary holes since this measurement is not needed to determine the manometer deflection as a function of flow rate.

The samples of powder used were either kaolins or grinding compounds. Five koalin samples, one aluminum oxide sample, and two emery powders were used. A description of the powders used appears in Table 1, including the source of supply. These powders were chosen since they were known to have very little internal surface area. It will be recalled that it was stated above that the permeability method was useful principally in determining external surface area.

Table 1. Description of Powder Samples

Sample	Material	Density ($\frac{gm.}{cm.^3}$)	Source	Surface ($\frac{m.^2}{gm.}$)
WH	Kaolin	2.58	Southern Clays, Inc. 33 Rector St. New York 6, N.Y.	7.6 *
WHRM-1	Kaolin	2.58	Southern Clays, Inc. 33 Rector St. New York 6, N.Y.	9.6 *
WHBM-1	Kaolin	2.58	Southern Clays, Inc. 33 Rector St. New York 6, N.Y.	8.9 *
WHBM-24	Kaolin	2.58	Southern Clays, Inc. 33 Rector St. New York 6, N.Y.	12.3 *
ASTM	Kaolin	2.58	Batelle Memorial Inst. 505 King Avenue Columbus 1, Ohio	5.3 **
1556-AB	Al_2O_3 Grinding Powder	4.0	Buehler, Ltd. 165 W. Waker Drive Chicago 1, Ill.	2.05 **
1560-S-AB	Emery, M-303 (800 mesh)	3.55	Buehler, Ltd. 165 W. Waker Drive Chicago 1, Ill.	0.73 **
1561-AB	Emery, M-303-1/2 (1200 mesh)	3.55	Buehler, Ltd. 165 W. Waker Drive Chicago 1, Ill.	1.22 **

* Indicates N_2 adsorption surface area determination by Micromeritics Laboratory, The State Engineering Experiment Station, Georgia Institute of Technology.

** Indicates area determined by P.T. Bankston using a dye adsorption method.

CHAPTER IV

PROCEDURE

Measurement of Powder Density.--For those powders not furnished with a density value for their solid form, the following technique was used to determine the density. A sample of the powder was inserted in a carefully weighed pycnometer bottle. The pycnometer and sample were weighed again on an analytical balance. The difference in these two weights was the weight of the powder. The pycnometer bottle was filled halfway with n butyl phthalate. The bottle containing the sample and the butyl phthalate were then connected to a vacuum. Care had to be taken at this point that a too-vigorous foaming did not carry away some of the sample. The connection to the vacuum served to draw air from the powder cake, and allow the butyl phthalate to wet the solid material. After no more bubbles were apparent, the pycnometer was filled completely with butyl phthalate and once again connected to a vacuum to draw off any air absorbed in the butyl phthalate. The top of the pycnometer was put in place, and the sample weighed once more. Thus the weight of the butyl phthalate, as well as the weight of the powder was determined.

The density of the butyl phthalate was measured by removing the powder sample and filling the pycnometer completely with deaereated butyl phthalate. The weight of the butyl phthalate divided by the nonimal volume of the pycnometer gave the density of the butyl phthalate. This figure, when divided into the weight of butyl phthalate required to

fill the pycnometer containing the powder sample gave the volume of the pycnometer not occupied by the powder. By subtraction of this volume from the pycnometer size, the volume of the powder sample could be determined. Therefore, knowing the weight and volume of the powder, the density could be determined. A sample calculation appears in the Appendix.

Preparation of the Packed Bed.--There has been much discussion in the literature concerning the proper method to use in order to get homogeneous packing in the bed. Various elaborate mechanical tamping devices which allow a weight to fall a given distance, a given number of times have been constructed. Some experimenters compact the entire sample in one stroke, while others compact in layers, adding a portion of the sample at a time. Lea and Nurse (8) present considerable evidence to show that very little difference can be detected between the results whether the beds have been packed in layers or in one stroke.

It was decided to use the one-stroke method of compaction, since this method was much more convenient. The sample was placed in the cylinder of the permeameter cell (see Figure 2) and the plunger fitted behind it in the cylinder. The cell, including the piston, was placed in a hydraulic press, advancing at the rate of three tenths of an inch per minute, and compressed to one hundred pounds. Several of the powders were pressed to three hundred and five hundred pounds, giving different porosities for the same powder.

Pressure Drop and Flow Measurements.--After packing the powder, the permeameter cell was connected in place in the permeameter assembly (see Figure 1). The vacuum pump, which supplied the vacuum to the

surge bottle, was turned on. Then by adjusting the air leak into the surge bottle, an approximate deflection could be set on manometer No. 1. When the manometers reached their equilibrium value, their levels were read with a cathetometer, and recorded. In order to insure that the liquid levels had reached their ultimate value, it was necessary to take cathetometer readings every 5 to 15 minutes until two or three consecutive readings gave the same value. At the extremely low flow rates used in several of the runs it took from two to three hours to attain an equilibrium reading. This reading was also sensitive to drafts in the room.

After one reading was made on a sample, several others were made at different manometer deflection values until the entire range of manometer No. 1 had been covered. Manometer No. 1 had a range limited by the lengths of the arms of the manometer (about 40 cm.). The range of manometer No. 2 could, in effect, be extended beyond its physical size by the use of a series of different sized capillaries. When the pressure drop across the bed per unit volume of gas permeating was large, the smallest capillary, made from a thermometer, was used to meter the flow. For beds of materials which offered less resistance to flow, it was necessary to begin with one of the small size capillaries for registering the low flow rates and then replace it with a larger size capillary in order to complete the range of pressure drops readable on manometer No. 1. After each equilibrium reading of the three manometers, the atmospheric pressure was determined with a mercury barometer, and the barometer reading corrected to 0° C.

Calibration of Capillaries.--The apparatus used to calibrate the flow

of air through the capillaries is shown in Figure 3. It was found that a second system was necessary in calibrating the thermometer capillary in the range of flows below 5.0 $cm.^3/hr$. The apparatus for this measurement is shown in Figure 4. For most of the calibrations the siphon arrangement shown in Figure 3 was satisfactory. The flow was adjusted by a screw clamp on the siphon tube. When the deflection on manometer No. 2 was steady, the amount of time it took to collect a given quantity of water in a graduated cylinder was measured. Several readings were made on manometer No. 2 while the sample was being collected. The average of these readings was taken as the manometer deflection, h_m, at the measured flow rate. It was assumed that the air above the water in the 24-liter bottle was saturated with water vapor at the surrounding temperature. By measuring the vacuum in the large bottle (with manometer No. 5) and knowing the barometric pressure, it was possible to calculate the moles of air drawn through the capillary in the time it took to collect the water sample. The 24-liter bottle was large enough in diameter so that the siphon head, and hence the flow rate and h_m, did not change appreciably during collection of the sample in the graduated cylinder.

At very low flow rates using the thermometer capillary, it was not possible to obtain a satisfactory calibration with the apparatus shown in Figure 3. The system shown in Figure 4 was capable of providing a more constant pressure driving air through the capillary. The procedure followed was to force air through the capillary by allowing mercury to drop slowly at a constant rate from the 100 ml. burette into the 2-liter bottle. This burette was filled to the 50 ml. mark, and the level maintained

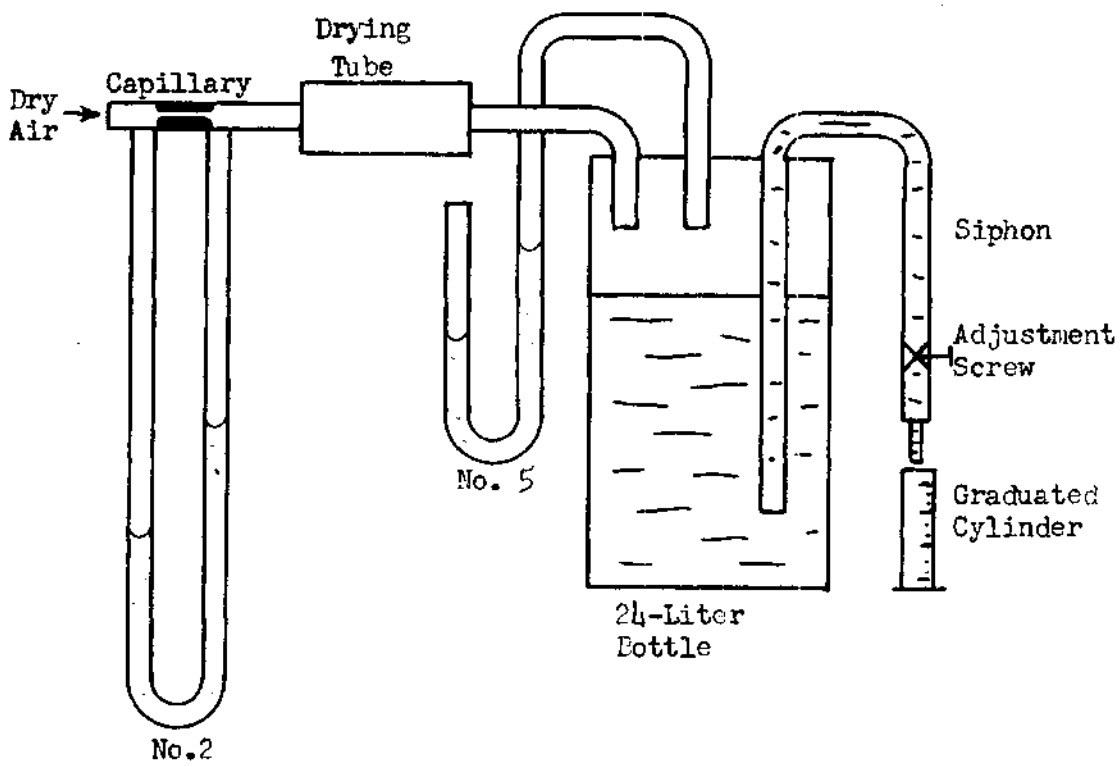

Figure 3. System for Capillary Calibration

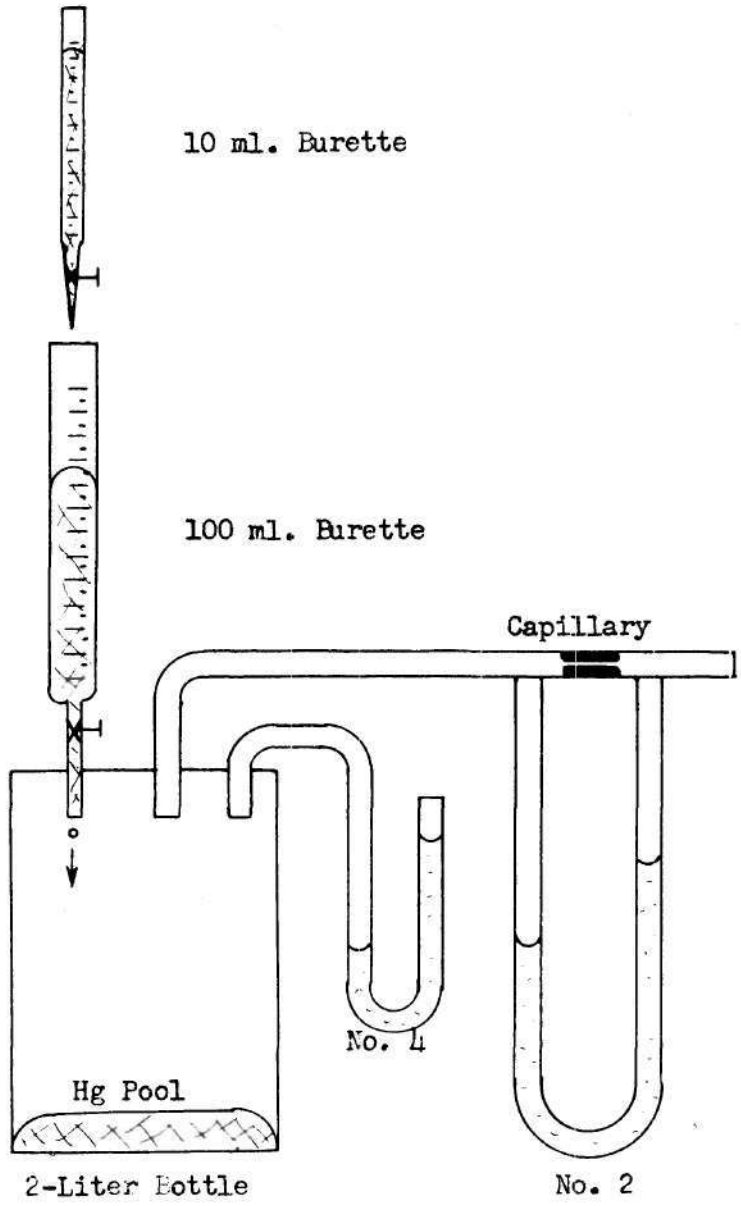

Figure 4. System for Thermometer Capillary Calibration at Low Flow Rates.

there by a continuous feed from a 10 ml. burette mounted about it. A small change in volume ($\pm$ 0.2 ml.) in the 100 ml. burette did not affect the rate of flow of mercury into the 2-liter bottle appreciably. Constant attention had to be given to the rate of flow out of the 10 ml. burette, however, in order to maintain the level in the 100 ml. burette within the limits indicated above. When the pressure in the bottle, and hence the flow through the orifice, became constant, a given quantity of mercury as measured on the 10 ml. burette was allowed to drop into the lower burette. The time this required gave the mercury flow rate. The volume measured on the 10 ml. burette was corrected if the volume in the 100 ml. burette changed during the timing process. At the same time, several readings were made on manometers (2) and (4). Again, knowing the absolute pressure in the 2-liter bottle, and the flow rate of mercury into the bottle, along with the surrounding temperature, it was possible to calculate the flow of gas through the capillary.

As a cross-check on the orifice calibrations, the two smallest capillaries, the thermometer capillary and the capillary designated /--/, were connected in series across monometers Nos. 1 and 2, shown in Figure 1. A vacuum was induced downstream by the vacuum pump and the monometer levels adjusted by the air leak into the surge bottle of Figure 1. Several readings were made, first with the thermometer capillary connected across manometer No. 1 and the capillary connected across manometer No. 2, and second with their positions reversed. The agreement was good.

CHAPTER V

DISCUSSION OF RESULTS

Comparative Results.--A summary of results is tabulated in Table 2. This table gives the dimensions of the bed, the porosity, and the surface area in square meters per gram as determined by various methods. Equation (14) is the Lea and Nurse equation derived above. Equation (36) is the Lyon equation, also given above. The Fanning friction factor - Reynolds number calculation of surface area will be given below. The B.E.T. figures given in the table are those obtained from nitrogen adsorption data using the Brunauer, Emmett, and Teller equation (19). These determinations were made at the Micromeritics Laboratory of the State Engineering Experiment Station of the Georgia Institute of Technology.

The surface area calculated by the Lea and Nurse equation is consistantly low by a factor of from two to six. This equation does not account for the change in density of the gas as it passes through the bed. Further, it makes no provision for Knudsen flow or "slip" at the walls of the pores in the bed. Both these effects are present, as will be shown below.

The Lyon Equation.--As will be recalled from the derivation of the Lyon equation (see Chapter II, THEORY, The Lyon Equation), the conductance function, F, when plotted as a function of $\overline{P}$, the average pressure in the bed, allowed for three conditions of flow. First, if the line had a positive slope and passed through the origin, the flow was said to be in

Table 2. Comparison of Results

Sample	Weight (gm.)	Bed Length (cm.)	ϵ	S_w in $m.^2/gm.$ Eq. (14)	Eq. (36)	f vs. N_{Re}	B.E.T.	$S_w = \frac{6}{D d_s}$ ***
WH	8.777	2.39	0.719	2.83	3.40	9.15	7.6	--
	8.777	2.28	0.706	2.82	3.56	8.40	7.6	--
	8.777	2.23	0.699	2.68	3.15	7.60	7.6	--
WHRM-1	10.199	2.47	0.683	3.30	4.19	8.25	9.6	--
	10.199	2.26	0.656	3.19	4.80	9.6	9.6	--
WHBM-1	9.209	2.26	0.687	3.02	4.05	8.44	8.9	--
	9.209	2.15	0.671	2.85	4.25	8.14	8.9	--
WHBM-24	9.764	2.06	0.639	3.67	7.42	8.32	12.3	--
ASTM	14.092	2.67	0.599	1.868	2.00	3.74	5.3 **	
1556 AB	20.202	3.50	0.715	1.678	2.77	5.55 *	2.05**	--
1560-S-AB	19.402	2.44	0.500	0.263	0.0577	0.374	0.73**	0.106
1561 AB	20.173	2.38	0.530	0.338	0.1037	0.466	1.22**	0.169

* This sample was extremely difficult to compact. It is believed that the measured porosity is greater than it should be. If a smaller porosity were used the surface area value determined by this method would be in better agreement with the dye adsorption value.

** Areas thus marked were determined by P.T. Bankston using a dye adsorption method.

*** Surface area values estimated by this method are usually somewhat low.

accordance with Poiseuille's law. Second, if the line had a positive slope, but had a finite intercept when $\bar{P}$ equals zero, then it was said that the flow was partially Poiseuillean and partly of the Knudsen type, resulting in a finite gas velocity at the wall ("slip"). The third condition was when the flow was entirely in the Knudsen region, and for that case the slope of F vs. $\bar{P}$ would be zero.

Figure 5 was taken from Knudsen's work with a single capillary (12). The results for one capillary should be comparable to a packed bed of powders, since the latter is assumed to contain a series of capillaries. The line marked P in Figure 5 is the expression of Poiseuille's law. The line marked K is the one in the Knudsen region. The solid line represents the data that was obtained. It is noted from Figure 5, that there is indeed a positive slope for flow in the region following Poiseuille's law, and that it does pass through the origin, if extrapolated. Also in the region where deviations from Poiseuille's law begin, a line could be drawn having a positive slope and intercept. It is in the region where the curve has a negative slope that the Lyon equation becomes incompatible with Knudsen's work with a single capillary. Equation (36) cannot accommodate a negative slope. The reason for this discrepancy is not clear.

Figures 6 through 13 show the author's work when treated in the same manner. It is noted that in no case did a positive slope appear. In fact several negative slopes are seen. On each curve is written an approximate D_c/λ value. This value is an estimation of the ratio of the mean pore diameter to the mean free path of the molecules in the gas.

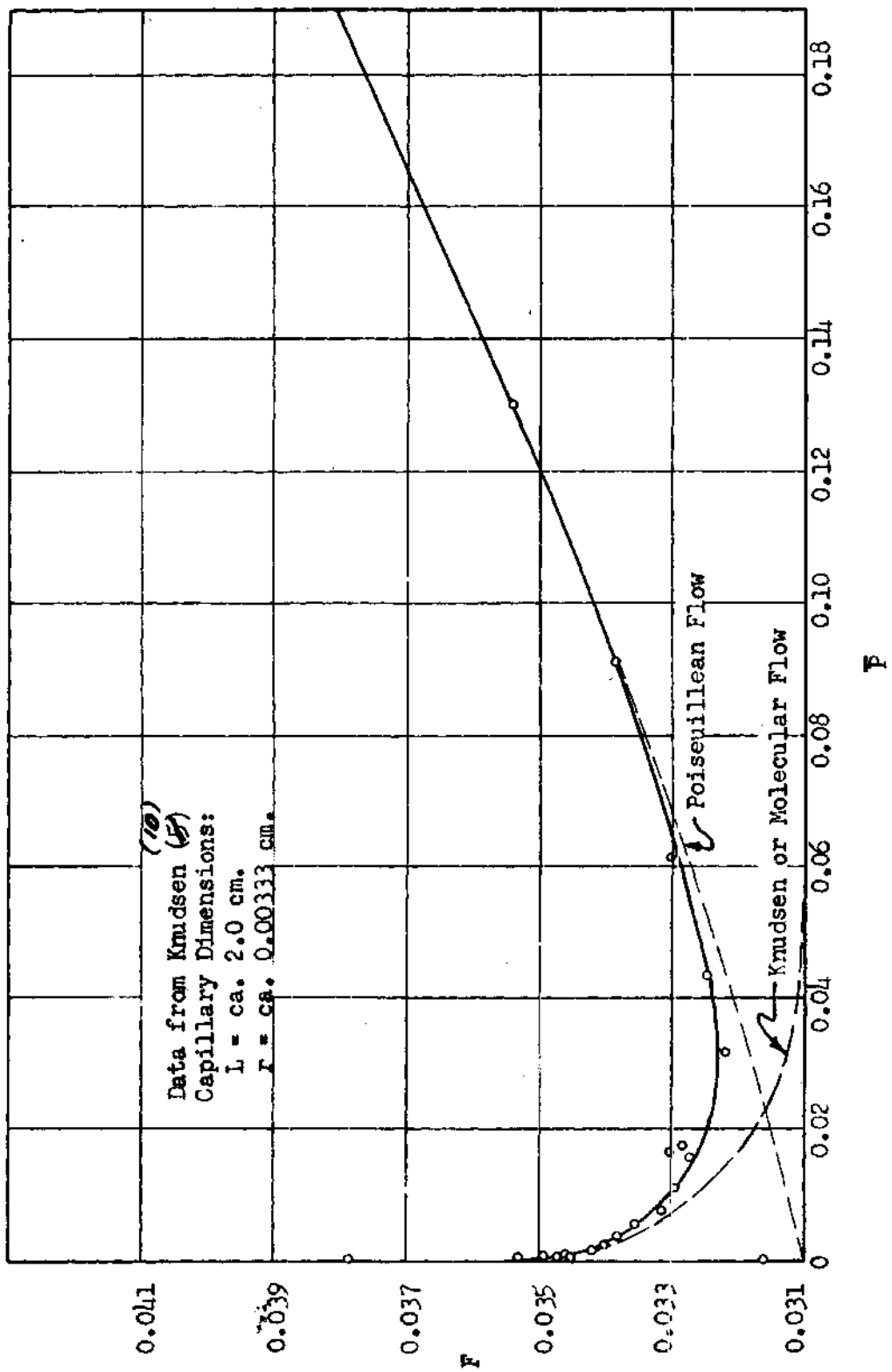

Figure 5. Flow of CO_2 Through a Single Capillary

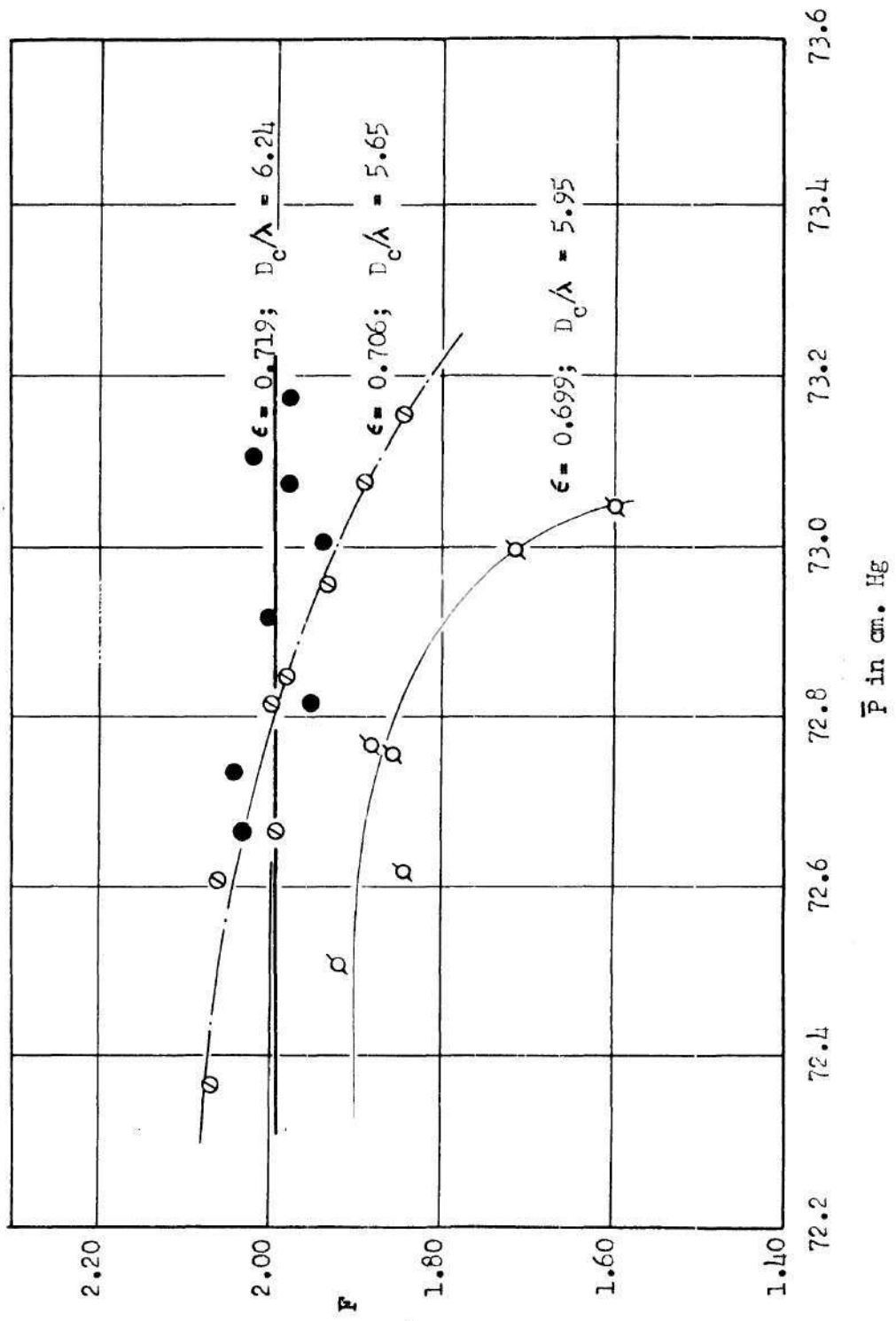

Figure 6. F vs. $\bar{P}$, WH Kaolin Sample

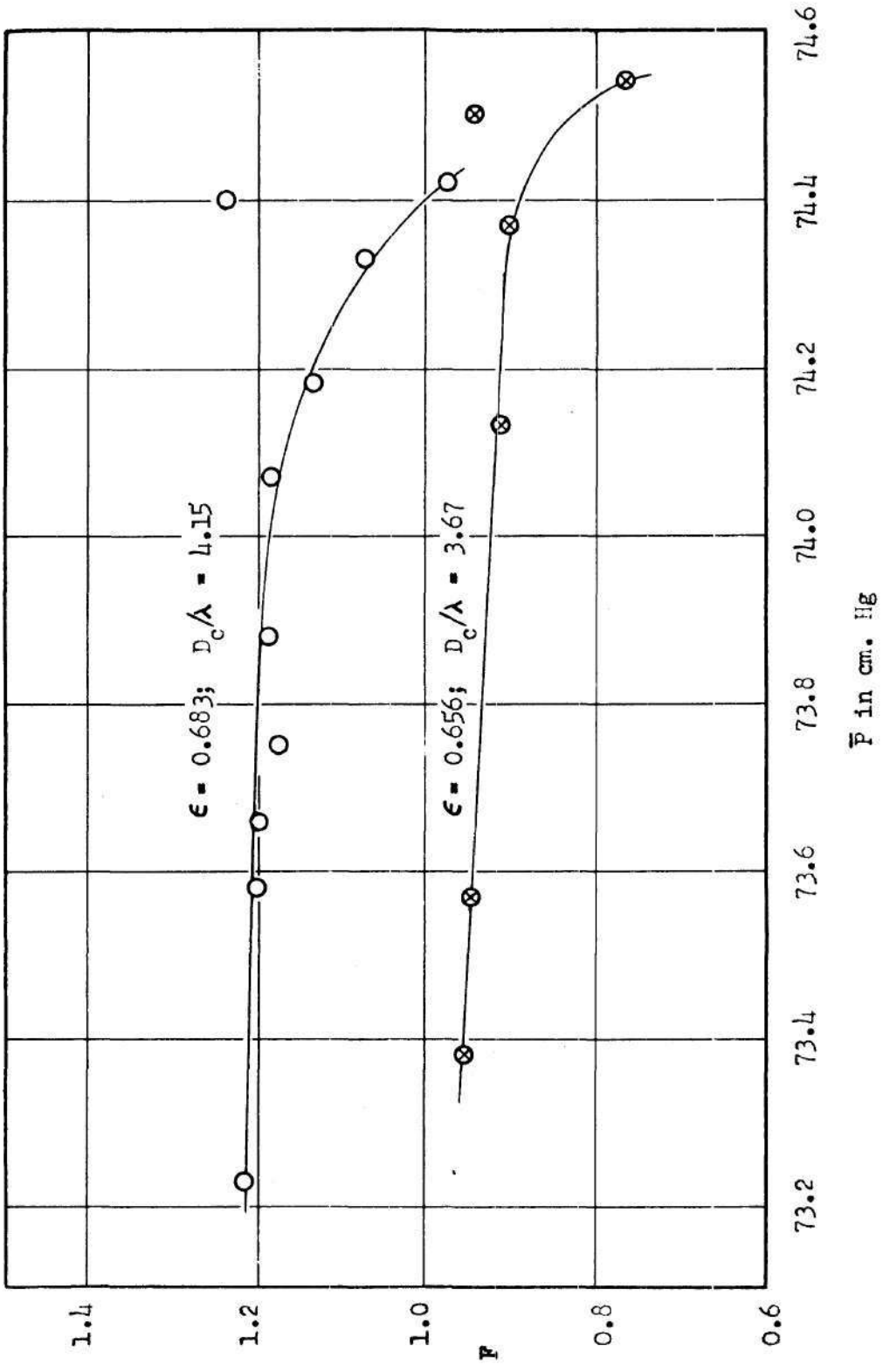

Figure 7. F vs. $\bar{P}$, NBRM-1 Kaolin Sample

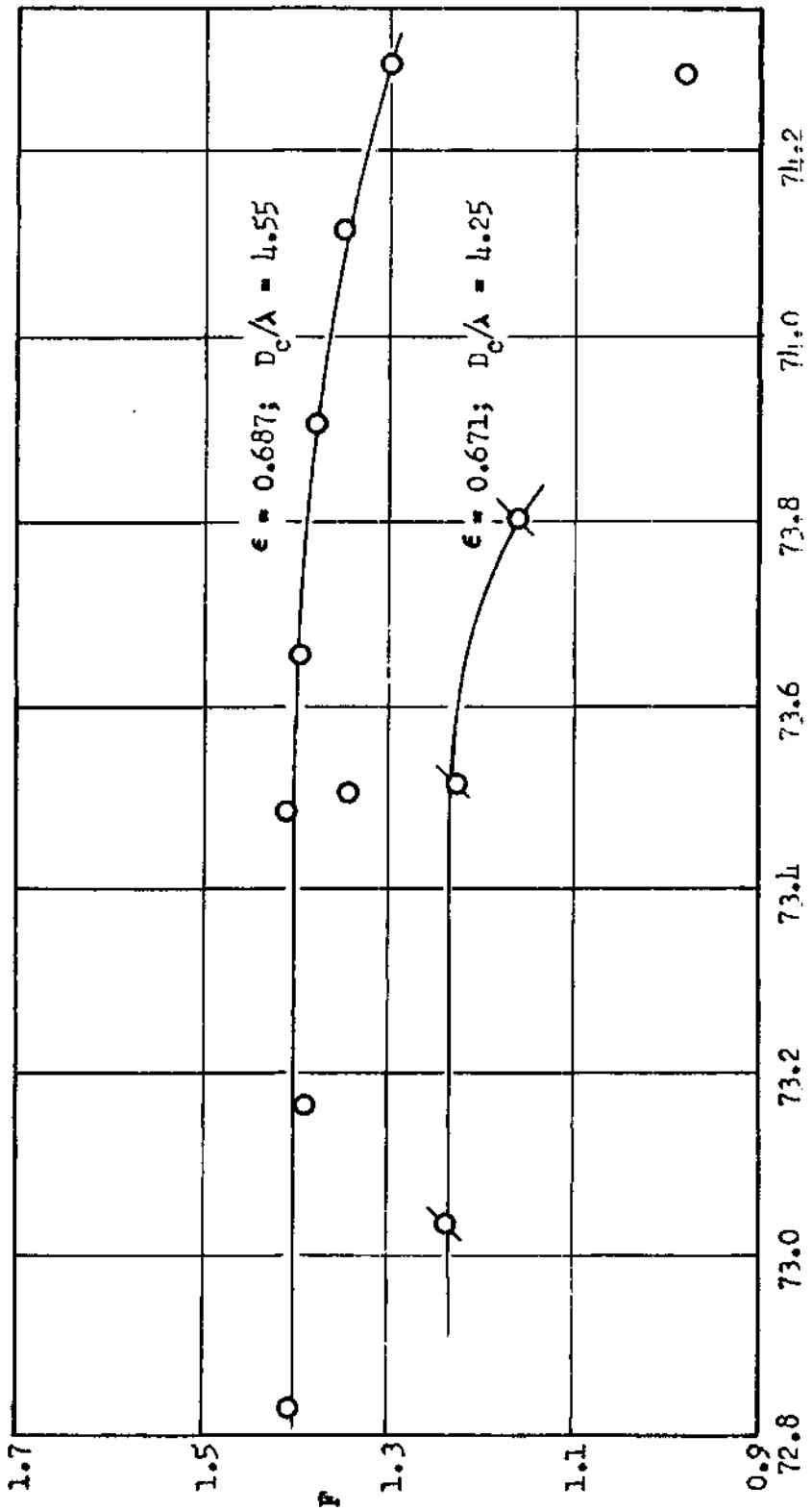

Figure 8. F vs. P̄, WHBM-1 Kaolin Sample

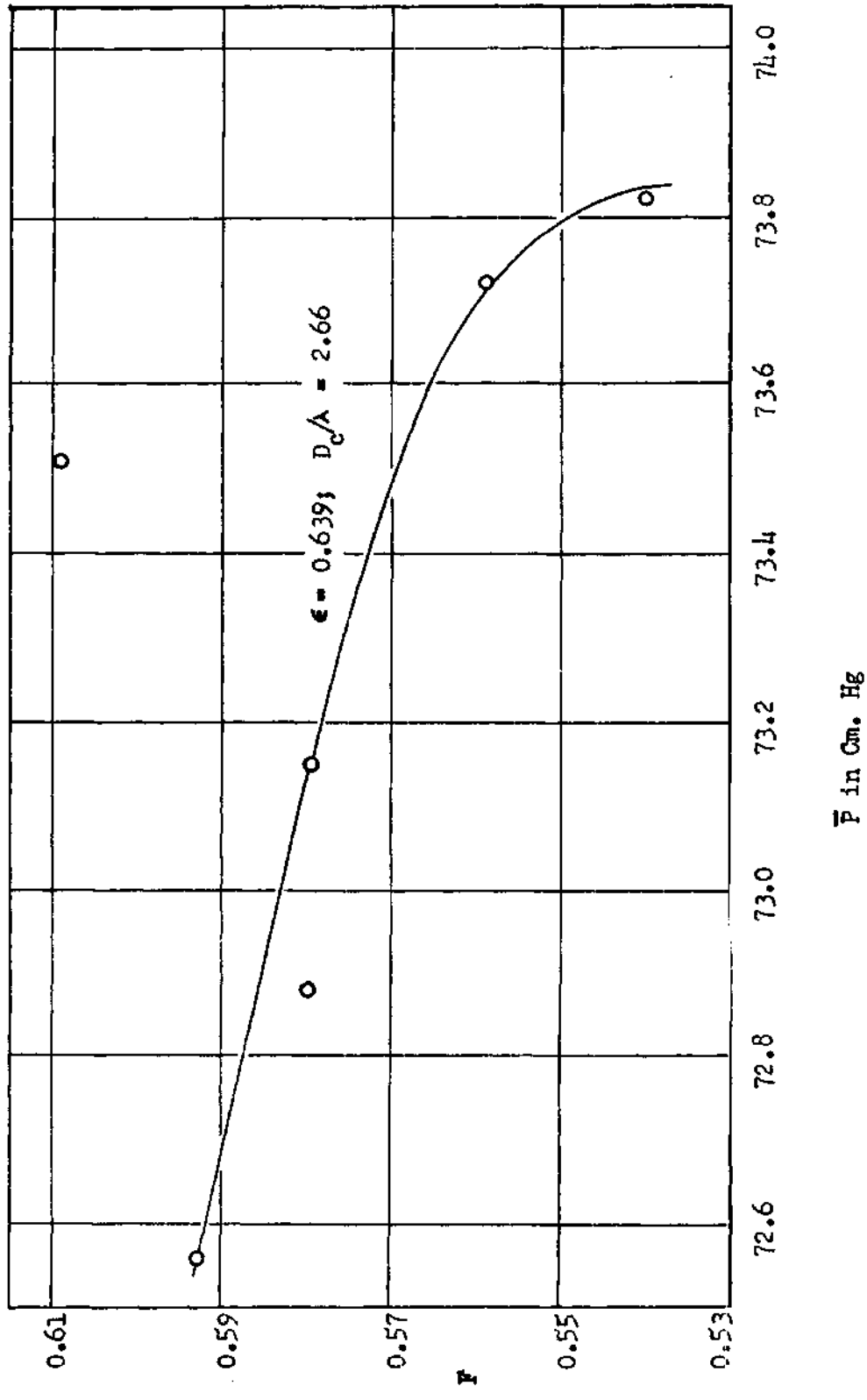

Figure 9. F vs. $\bar{P}$, UHBM-24 Kaolin Sample

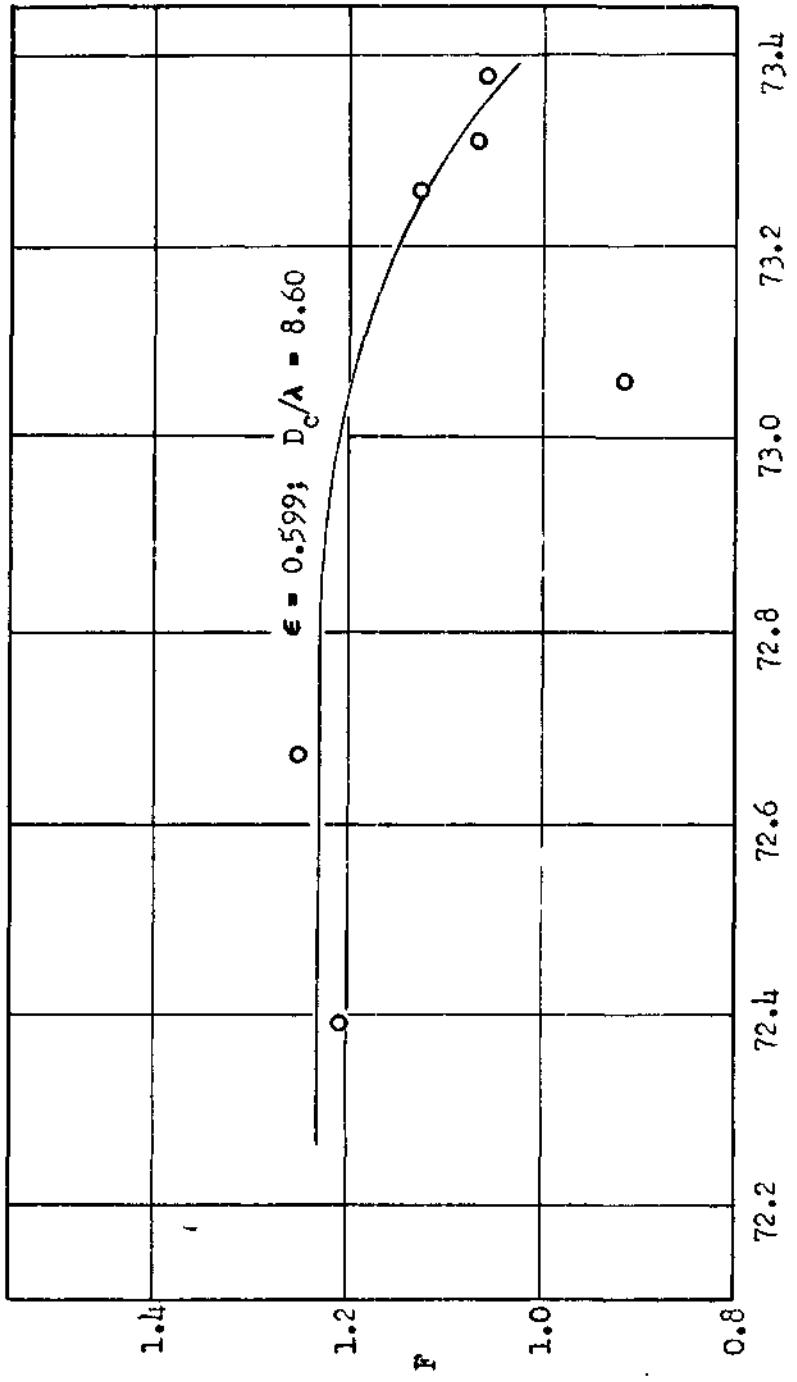

Figure 10. F vs. $\bar{P}$, ASTM Kaolin Sample

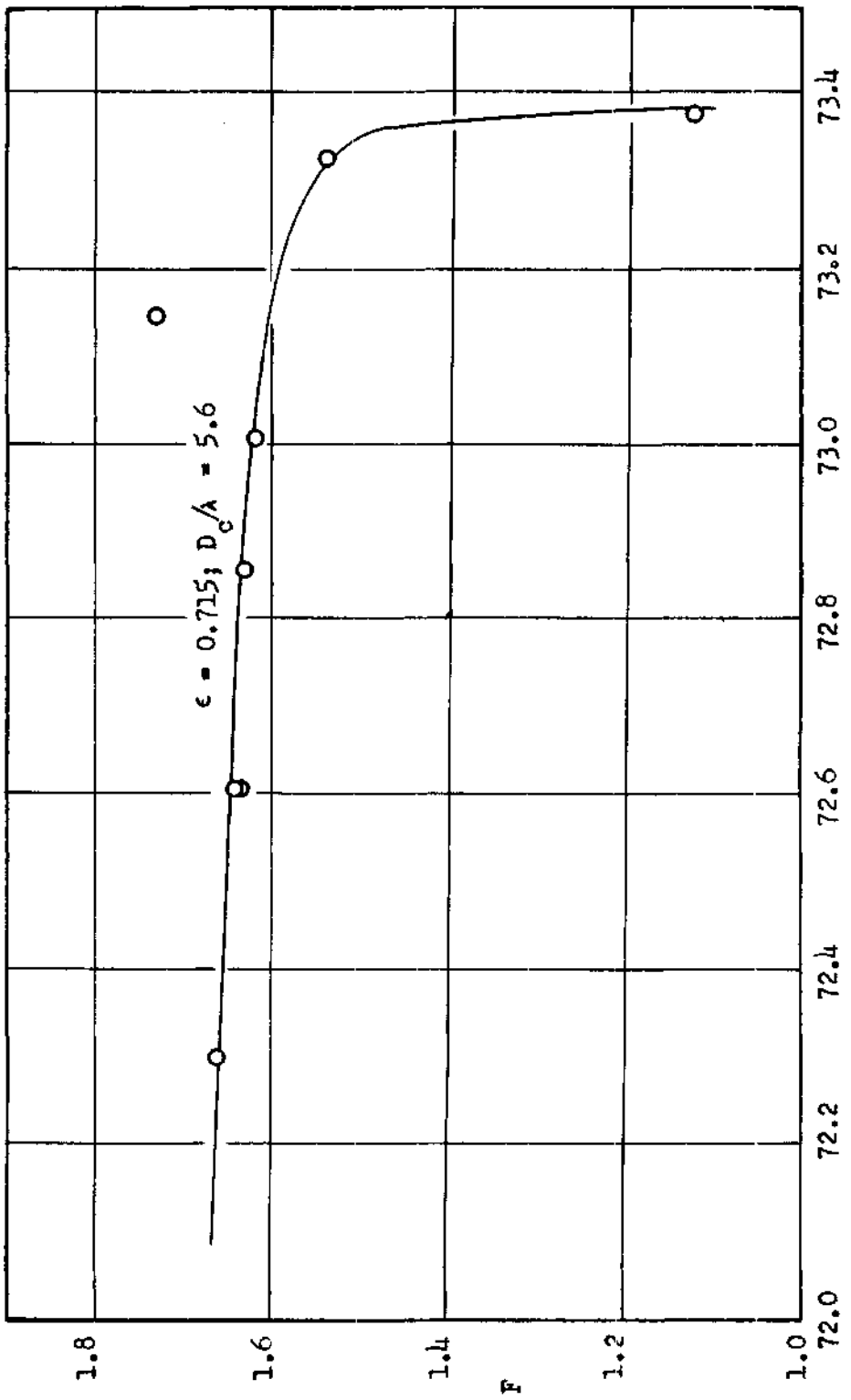

Figure 11. F vs. $\bar{P}$, 1556-AB Al_2O_3 Grinding Powder

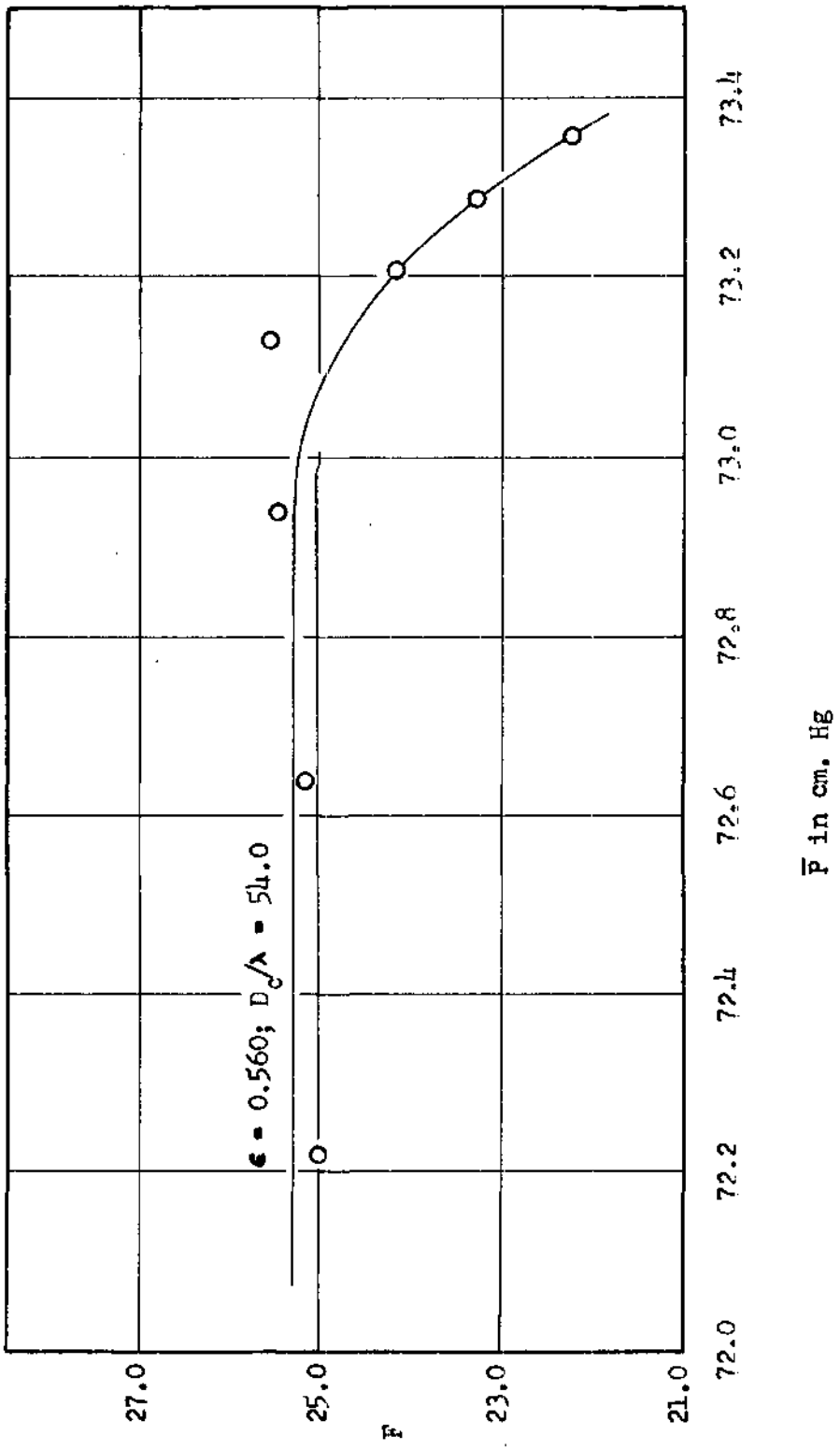

Figure 12. F vs. $\bar{P}$, 1560-S-AB Emery Grinding Compound

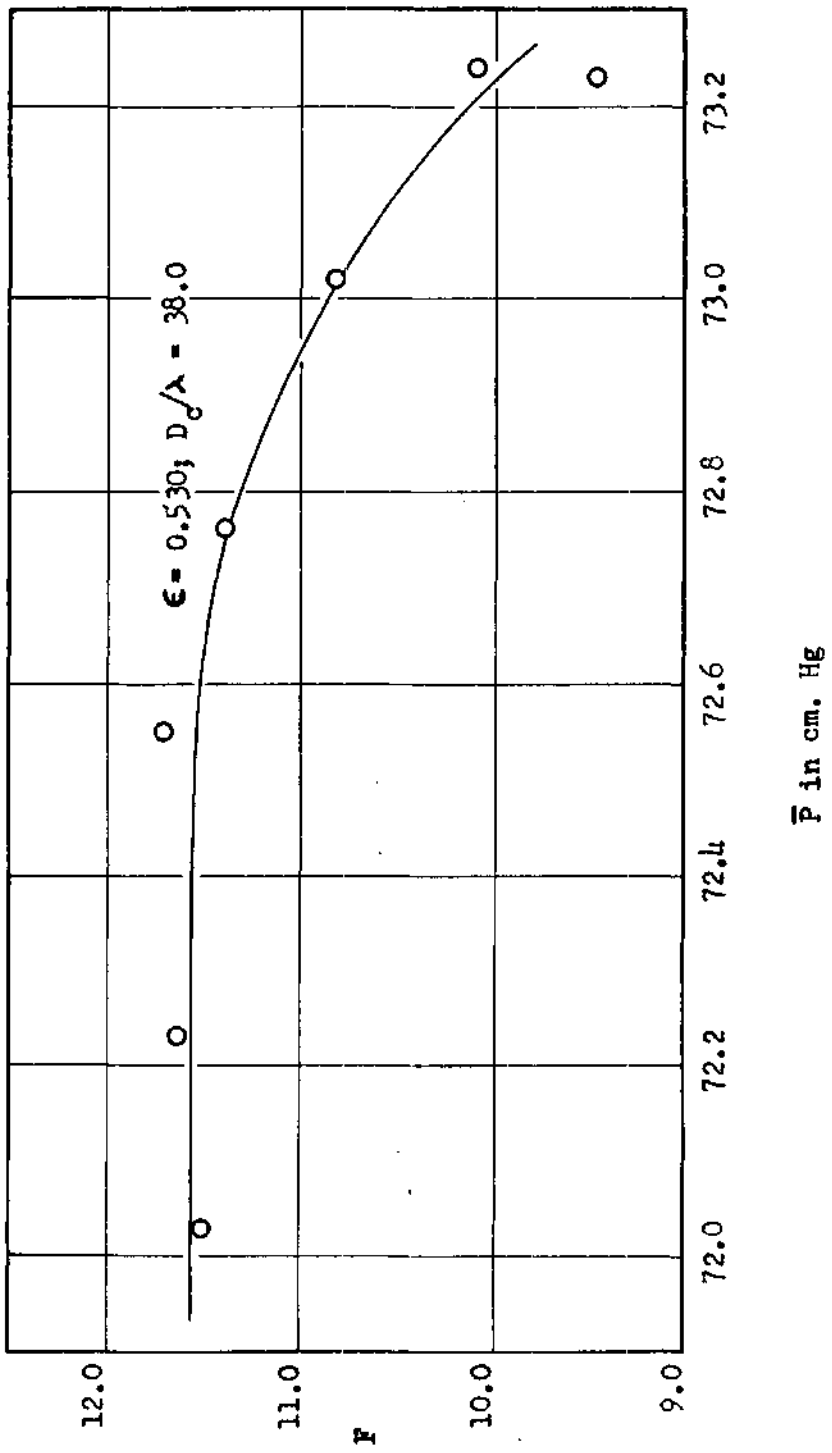

Figure 13. F vs. P, 1561-AB Emery Grinding Compound

The pore diameter, D_c, was estimated by equation (43), and the mean free path, λ, over the pressure and temperatures involved was taken constant at 9.5×10^{-6} cm.

Further study of Figures 6 through 13 indicates that as the ratio of D_c to λ becomes smaller, for each sample, the negative slope increases, indicating a closer approach to free molecule flow. This effect can also be seen from sample to sample. For example, Figures 9 and 10 can be compared. In Figure 9, the ratio has a value of 2.6, while for Figure 10 the ratio is 8.6. For those samples which display a zero slope to the F vs. $\overline{P}$ cure, it is believed that slip is occurring at the walls, in the light of the information contained in Figure 5.

The discussion as to why the curves have a convex curvature upward, and drop sharply at $\overline{P}$ values close to atmospheric pressure will be deferred momentarily. For each of the curves of Figures 9 through 13, a horizontal line has been drawn through the points on the flatter portion of the curve. It was the intercept value of this line that was used, along with equation (36), to calculate S_w by the Lyon method. A zero slope was assumed in these calculations.

The Low Flow-Rate Phenomenon.--In Figures 7 through 13, there is a noticeable, abnormal drop in F as $\overline{P}$ approaches atmospheric pressure. At these values of $\overline{P}$ there is a very small velocity of gas passing through the bed. There is also very little deflection on the manometers in this region. Therefore the accumulative errors represented by these points can be large, making the points appear low when they should not actually be so.

The fact that this effect occurred for every sample deserves some additional attention. This dropping-off of F is just the opposite of what occurs in the free molecule flow region. If it is assumed that the phenomenon actually exists, then it remains to reason why. Either Q is decreasing disproportionately, or $(P_2 - P_1)$ is increasing in the same manner. In either case there would seem to be an added resistance to flow. It may be that at the low flow rates, and hence low shear stresses, experienced by the gas, that the coefficient of viscosity is no longer a constant; that is, it may increase at the low shear stresses. In any case it seems worthwhile to investigate the phenomenon further.

The Reduced Fanning Friction Factor-Reynolds Number Relation.--The $f = \phi N_{Re}$ relation may be expressed in terms of the surface area per unit mass by substitution of equation (43) into equation (48). The result is:

$$\left\{\frac{\Delta hg \cdot 4\epsilon}{2u^2 L(1-\epsilon)d_s}\right\}\frac{1}{S_w} = \phi\left[\left\{\frac{4\epsilon^4 ud}{(1-\epsilon)^3 \mu d_s}\right\}\cdot\frac{1}{S_w}\right] \qquad (49)$$

Figure 14 is a graph of this function, using the surface area as calculated by the Lyon equation. It includes only those powders for which the surface area was known as determined by the nitrogen adsorption method. Figure 15 shows these same points plotted using the nitrogen adsorption surface area instead of that determined by permeability methods. A line was then drawn which represented these points. This line is called a "reduced line" being the line to which the data was reduced when using the nitrogen adsorption value for the surface area in equation (49). It is then assumed that the reduced line is unique for all packed materials which do not have large internal areas. The equation

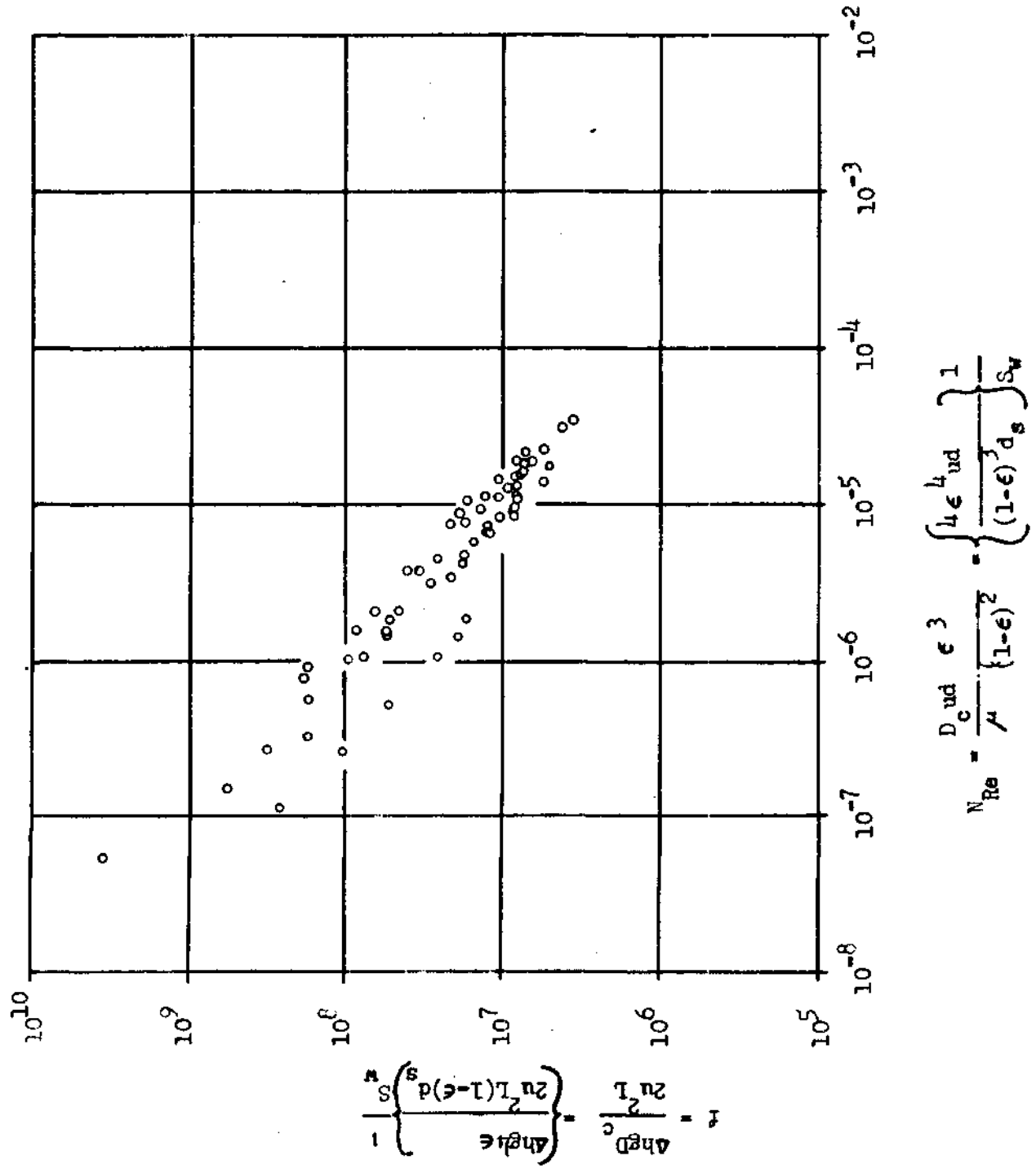

Figure 14. f vs. N_{Re}, Selected Powders

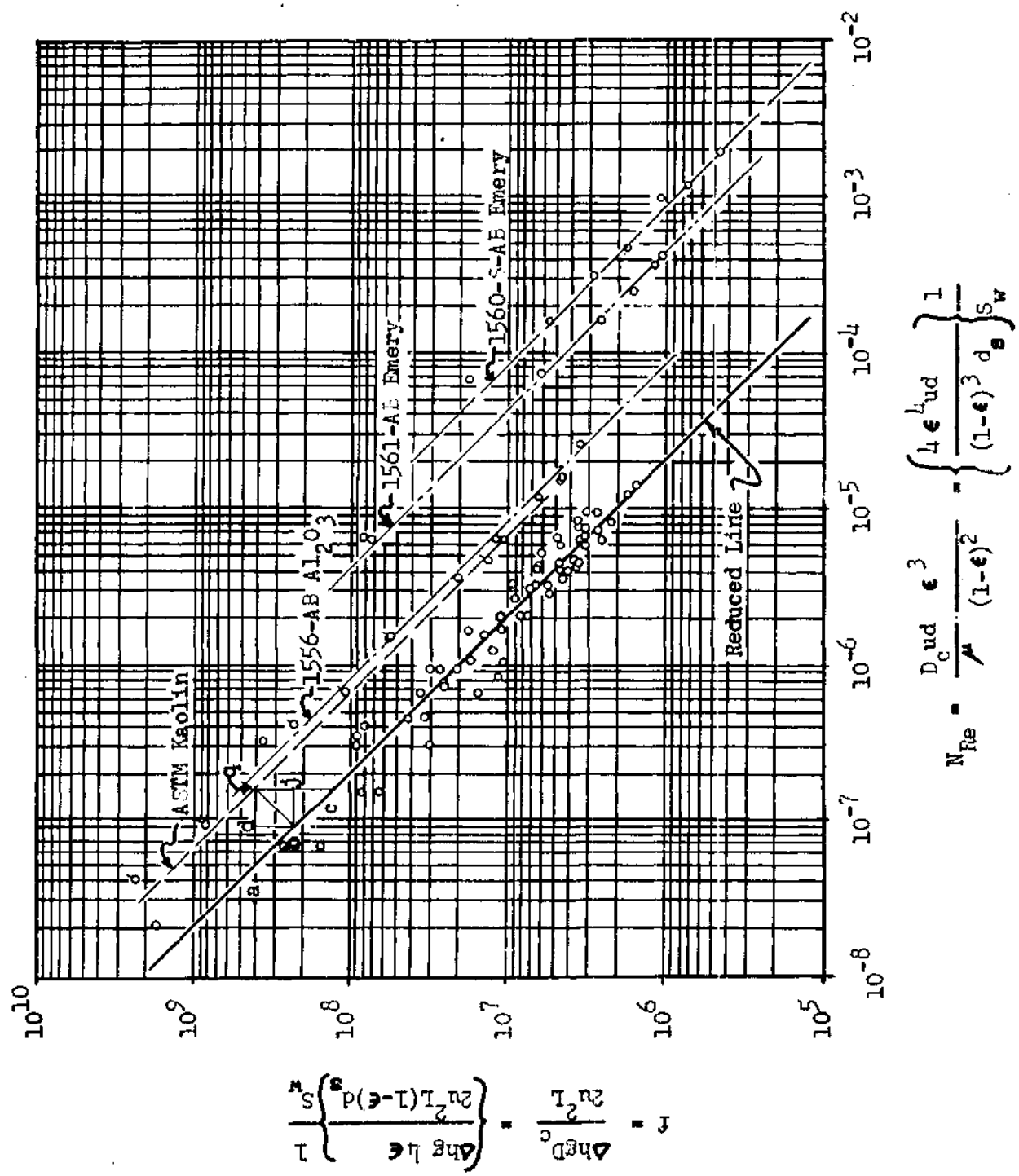

Figure 15. f vs. N_{Re} , Reduced to Nitrogen Adsorption Surface Areas

for the reduced line is

$$f = \frac{21.9}{N_{Re}} \tag{50}$$

Samples for which no nitrogen adsorption data exists may be converted to the reduced line in the following manner. The short-dashed line drawn on Figure 15 represents the permeability data for the ASTM Kaolin sample. The surface area value used to construct this line was that calculated from the Lyon equation. Actually the Lea and Nurse equation would have been satisfactory to use in constructing the line. Further, an arbritrary value of 1.0 could have been used for S_w with the same result. Refer to point q on the ASTM line. If a perpendicular is constructed from point q to the reduced line intersecting at b, then,

$\frac{f_q}{f_j}$ = the factor by which S_w (the S_w used to construct the dashed line) must be multiplied to make both lines coincident.

Also the product

$$\frac{f_q}{f_j} \times (S_w) \text{ permeameter} = S_w,$$

which is a better estimation of the external surface area.

The other dashed lines, based on the Lyon value for S_w, in Figure 15 were reduced by the same method to give the surface area values shown in Table 2 in the f vs. N_{Re} column.

It was not possible to apply this method, based on the Fanning friction factor-Reynolds number relation, to other samples given in the literature because the data are insufficient.

CHAPTER VI

CONCLUSIONS

The following conclusions were drawn from this study:

1. The Lea and Nurse equation, equation (14), is unsatisfactory in calculating the surface area of particles by the permeability method.

2. The Lyon equation, equations (35) and (36), is not entirely satisfactory in describing the flow of a gas through a porous medium.

3. Calculation of the surface area of a finely divided material by means of the Lyon equation is unsatisfactory.

4. The permeability data may be correlated by using the Fanning friction factor and a modified Reynolds number, equation (48), or equation (49).

5. The relation cited in 4 may be reduced to a unique function by utilizing the surface area determined by nitrogen adsorption methods. This function is $f = 21.9/N_{Re}$.

6. The procedure for using the Fanning friction factor-Reynolds number relation based on known values of surface area gives a better representation of the premeability data and more accurate values of the external surface area of finely divided materials.

7. At very low rates of flow there is an added resistance, not accounted for in the standard equations describing flow.

CHAPTER VII

RECOMMENDATIONS

1. It is recommended that the Friction Factor - Reynolds Number relation derived be extended over a larger range. Use of a larger range of porosities and specific surface areas in this extension is suggested.

2. The results indicating that there is an added resistance to flow occurring at very low flow rates should be further investigated.

APPENDIX

APPENDIX A

LITERATURE CITED

1. Lea, F.M. and Nurse, R.W. J. Soc. Chem. Ind., 58 (1939), p. 277.
2. Gooden, E.L. and Smith, C.M. Ind. Eng. Chem., 12 (1940), p. 479.
3. Rigden, P.J. J. Soc. Chem. Ind., 62 (1943), p. 1.
4. Ibid., 66 (1947), p. 130.
5. Carman, P.C. Trans. Inst. Chem. Engrs., London, 15 (1937), p. 150.
6. --., J. Soc. Chem. Ind., 57 (1938), p. 225.
7. Ibid., 58 (1939), p. 1.
8. Lea, F.M. and Nurse, R.W. "Permeability Methods of Fineness Measurement," Symposium on Particle Size Analysis, London: Inst. of Chem. Engrs., 1947. pp. 47-57.
9. Meyerott, R. and Morgenau, H. Amer. J. Sci., 243 (1949), p. 192.
10. Knudsen, M. Ann. Physik., 28 (1909), p. 75.
11. Ibid., 35 (1911), p. 389.
12. Ibid., 28 (1909), pp. 101, 2.
13. Gaede, W., Ann. Physik., 41 (1913), p. 289.
14. Bates, P.H. "Report on Air Permeability Methods for Determining Fineness of Cement," A.S.T.M. Bulletin No. 118, (1942), p. 31.
15. Lea, F.M. and Nurse, R.W., "Portland Cement," Bureau of Standards Institution Circular No. 12, London, 1947.
16. --. J. Soc. Chem. Ind., 58 (1939), p. 225T.
17. Sullivan, R.R. and Hertel, K.L. Advances in Colloid Science Vol. I. New York: Interscience Publishers, 1942. p. 37.
18. Lyon, L.L. and Others. The Permeability Method of Determining Surface Areas of Finely Divided Materials. Wichita: University of Wichita Foundation, 1951.

19. Brunauer, S. The Adsorption of Gases and Vapors. Vol. I, Physical Adsorption. Princeton: Princeton University Press, 1943.

20. Arnell, J.C. Canadian Journal of Research, A24 (1946), p. 103.

21. Ibid., A25 (1947), p. 199.

22. Herzfeld, K.F. and Smallwood, H.M. Taylor's Treatise on Physical Chemistry. Vol. I. 2nd ed.; New York: D. Van Nostrand Co., Inc.,

23. Pollard, W.G. and Present, R.D. Physical Review, 73 (1948), p. 762,

24. Bosanquet, C.H. British TA Report BR-507, September 27, 1944.

25. McAdams, W.H. Heat Transmission. 2nd ed.; New York: McGraw-Hill Book Company, 1942, p. 90.

APPENDIX B

NOMENCLATURE

A	the total cross sectional area of the bed, square centimeters
Al_2O_3	aluminum oxide
B.E.T.	Brunauer, Emmett, and Teller method of determining surface areas by nitrogen adsorption
C	a constant for the capillary flowmeter, $cm.^4/sec.^2$
$^oC.$	degrees centigrade
cm.	centimeters
D	the diameter, centimeters
D_c	the diameter of the capillary, centimeters
d	the gas density, grams per cubic centimeter
d_m	the density of the manometer fluid, grams per cubic centimeter
d_s	the solid density of the material composing the bed, grams per cubic centimeter
F	the fluid conductance, equal to the flow rate (QP_1) per unit pressure drop, cubic centimeters per second
f	the Fanning friction factor equal to $\frac{\Delta h g}{2u^2 L(1-\epsilon)d_s} \cdot \frac{1}{S_w}$ in terms of permeability data, dimensionless
G	the total grams of gas transported
g	the acceleration of gravity, centimeters per second per second
gm	grams
h_1	difference in level of liquid in the manometer measuring pressure difference across the bed of material, centimeters
h_2	difference in level of liquid in the manometer measuring pressure difference across the capillary, centimeters

Δh pressure head equal to $\frac{-\Delta P}{dg}$, centimeters

Hg chemical symbol for mercury

hr. hour

K, K' arbitrary constants

K_1 a constant pertaining to viscous flow

K_2 a constant pertaining to free molecule flow

k a shape factor, Carman's constant equal to 5.0, dimensionless

L the length of the packed bed, centimeters

L. liter

M the molecular weight, grams per gram mole

m the mass of one molecule, grams

m the hydraulic radius, centimeters

m. meters

N the number of capillaries in a porous medium

N_{Re} the Reynolds number, dimensionless

n a number of molecules

P_1, P_2 the pressure upstream and downstream of the bed, respectively, dynes per square centimeter

$\bar{P}$ the average pressure in the bed, equal to $\frac{P_1+P_2}{2}$, dynes per square centimeter

ΔP the pressure drop across the bed, equal to $\frac{P_1-P_2}{2}$, dynes per square centimeter

Q the rate of flow through the bed, cubic centimeters per second, measured at P_1

R the molal gas constant, equal to 8.3136×10^7 ergs per degree Kelvin per gram mole

r the radius of capillary, centimeters

S_t	the total surface area of the solid, square centimeters
S_v	the specific surface area of the solid, square centimeters per cubic centimeter of solid material
S_w	the specific surface area of the solid, square centimeters per gram
Sec.	Second
s.t.p.	at standard temperature (0°C.) and pressure (76.0 cm. Hg)
T	the temperature of the gas flowing through the bed, degrees Kelvin or centigrade
u	the superficial velocity, the velocity of the gas as if it were flowing through an empty permeameter cell, centimeters per second.
u_c	the velocity through a capillary, centimeters per second
V_s	the solid volume, cubic centimeters
V_t	the total volume, cubic centimeters
V_v	the void volume, cubic centimeters
$\bar{v}$	the mean molecular speed, centimeters per second
w_s	the weight of the sample, grams
x	the direction of flow
$\bar{\Gamma}$	the average number of molecules flowing per unit time
ϵ	the porosity, void volume divided by the total volume, dimensionless
λ	the mean free path of the gas, centimeters
μ	the viscosity of the gas, poise
π	pi, 3.1416, dimensionless
ϕ	any function of the argument

APPENDIX C

CAPILLARY CALIBRATIONS

The rate of flow through the flowmeter is given by

$$Q = \frac{C\, h_2\, d_m}{\mu} . \qquad (11)$$

Therefore $Q = \phi\, h_2$

The Q plotted in Figures 16, 17, and 18, is reported in liters/hr. at standard pressure and temperature.

A sample calculation will be shown for the point at h_2 = 2.41 for capillary designated /-/. Reference is directed to Figure 3 for the experimental set-up.

Experimental Data:

h_2	Vac. (in bottle)
= 6.42	= 5.31
= 6.41	= 5.31
= 6.41	= 5.29
= 6.41	= 5.29
Ave. h_2 = 6.41 cm. red oil	Ave. vac. = 5.30 cm. H_2O

T_a = 300.6°K, P_b = 743.4 mm. Hg (corrected to 0°C.)

Size of water sample = 9.0 cc

Time for collection of sample = 234.0 sec.

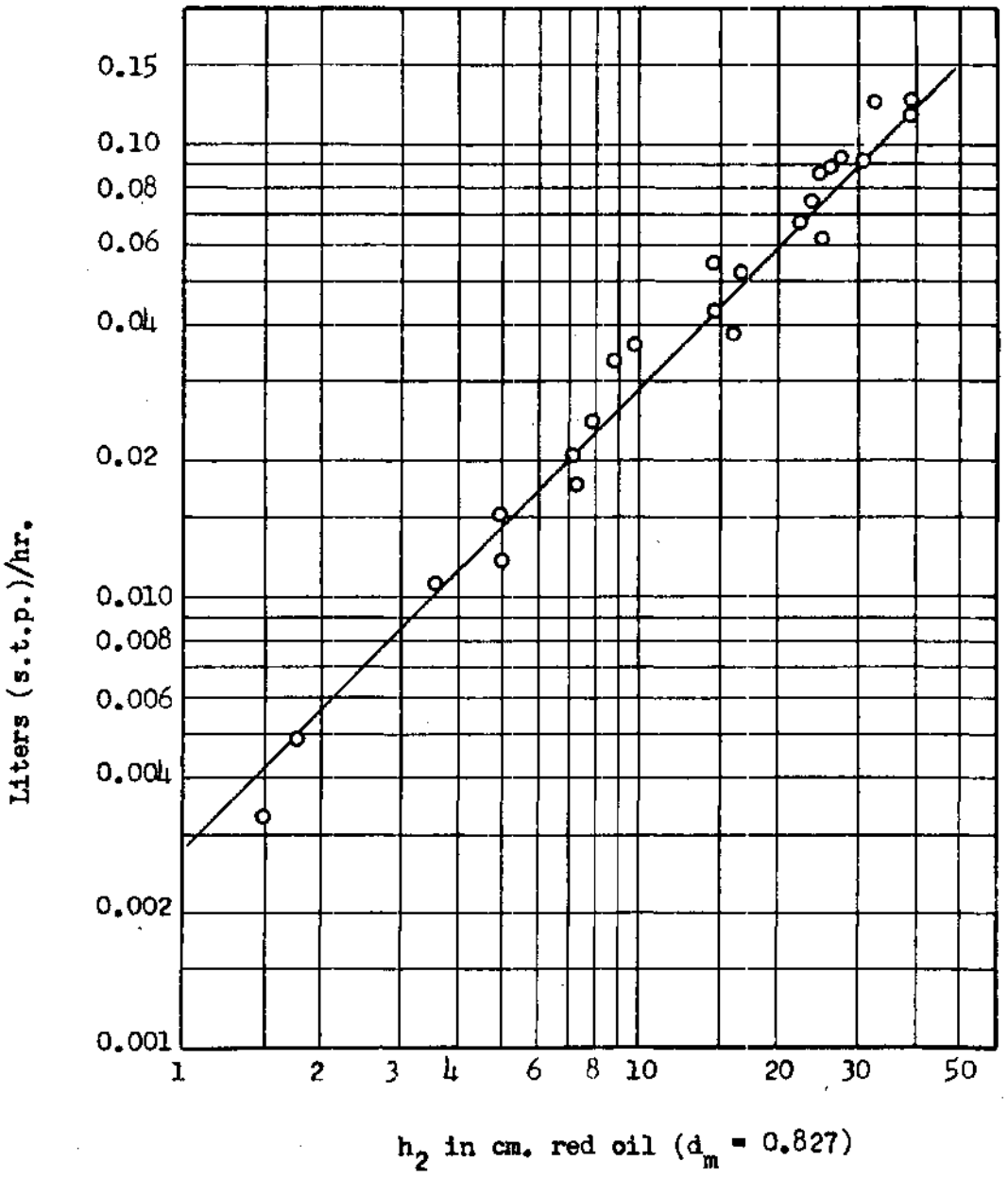

Figure 16. Capillary Calibration, Thermometer Capillary

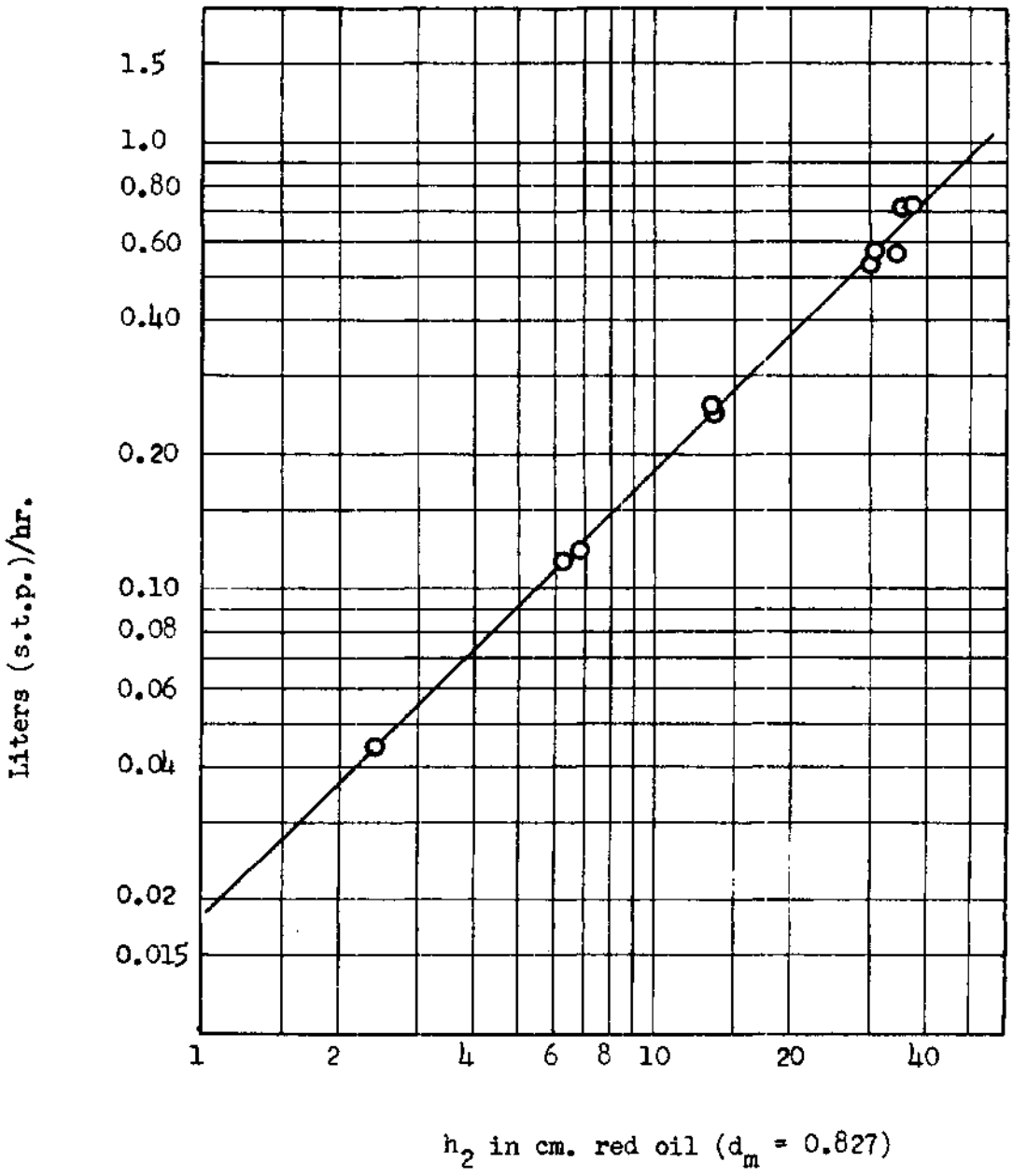

Figure 17. Capillary Calibration, /--/ Capillary

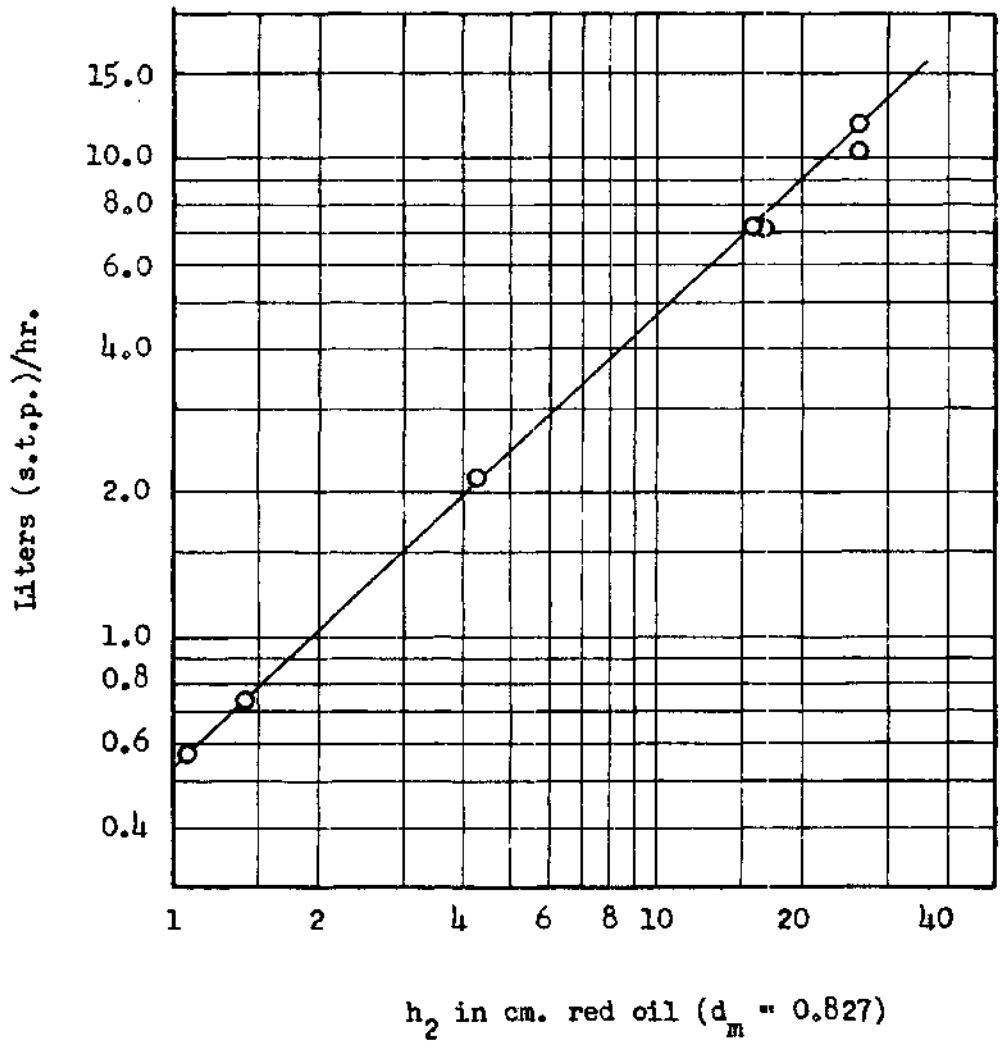

Figure 18. Capillary Calibration, No. 11 Capillary

Calculations:

$$\text{vacuum in bottle} = 5.30 \text{ cm. } H_2O \frac{0.995 \text{ gm./cm.}^3 H_2O}{13.59 \text{ gm./cm.}^3 Hg} \times 10 \text{ mm./cm.}$$

$$= 3.9 \text{ mm. Hg}$$

pressure in bottle = 743.4 - 3.9 = 739.5 mm. Hg.

Moles of air in bottle equivalent to 9.0 cc H_2O removed

$$n = \frac{PV}{RT} = \frac{\frac{739.5}{760.0} \cdot 9.0}{82.06 \cdot 300.6} = 3.55 \times 10^{-4} \text{ moles}$$

humidity at 27.5°C., 100% relative humidity

$$= 0.038 \frac{\text{moles of water vapor}}{\text{mole of bone dry air}}$$

Basis: 1 mole of bone dry air

1.000 moles dry air

0.038 moles water vapor

1.038 moles wet air

Therefore in 3.55×10^{-4} moles of wet air, calculate the water vapor as

$$\frac{0.038}{1.038} 3.55 \times 10^{-4} = 0.13 \times 10^{-4} \text{ moles of water vapor.}$$

Therefore,

$(3.55-0.13) \times 10^{-4} = 3.42 \times 10^{-4}$ moles of bone dry air drawn through the capillary.

At standard temperature and pressure,

$V = n \times \text{molal volume (s.t.p.)} = (3.42 \times 10^{-4}$

$V = 7.66 \times 10^{-3}$ L. (s.t.p.)

Therefore, $Q = \frac{7.66 \times 10^{-3} \text{L. (s.t.p.)}}{234.0 \text{ sec.}} \times 3600 \text{ sec./hr.}$, or

$$Q = 0.1188 \quad \text{L (s.t.p.)/hr.}$$

The calculation using mercury upstream to drive the air through the capillary is similar except the amount of mercury vapor is considered negligible.

APPENDIX D

EXPERIMENTAL DATA

The following diagram and symbols serve to define the meaning of the symbols appearing in the tables of experimental data.

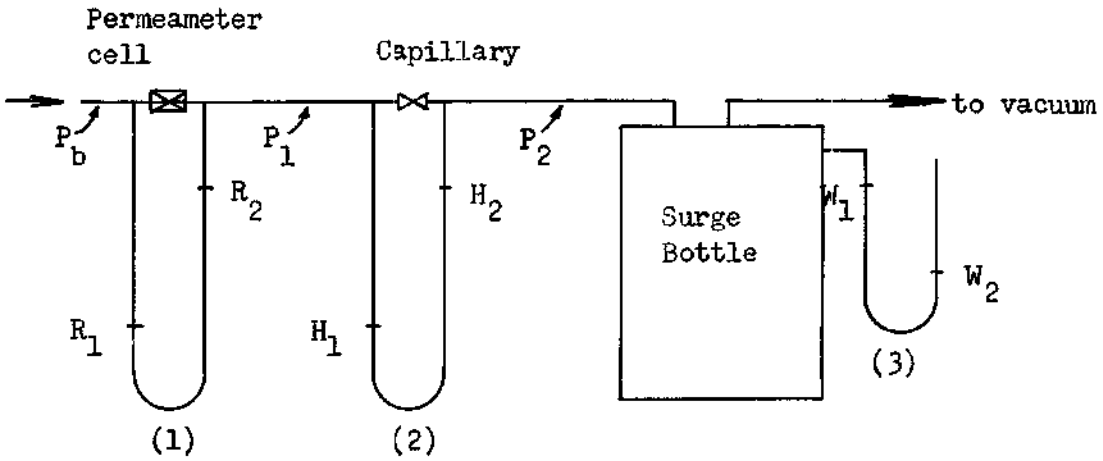

d_m = manometer fluid density, manometers (1) and (2) = 0.827gm./cm.^{3}

R_2-R_1 = Δ P across bed in centimeters manometer deflection

H_2-H_1 = h_m

W_1-W_2 = Vac.

T_a = Temperature of the permeameter apparatus

P_b = barometric pressure, corrected to 0°C.

L = length of bed; V_t = total volume of bed; V_s = volume of solids

w_s = weight of sample; d_s = density of solid material

ϵ = porosity

P_1,P_2 = pressure upstream and downstream of capillary, respectively

Capillaries (cap.):

(1) Th Thermometer

(2) /--/ Intermediate

(3) 11 No. 11

Table 3. Experimental Data, WH Kaolin Sample

d_s = 2.58 gm./cm.^{3}

W_s = 8.7772 gm. ; V_s = 3.402 cm.^{3}

Pressed to 100 lbs. ; L = 2.385 cm. ; V_t = 12.10 cm.^{3} ; ϵ = 0.719

Run	Cap.	R_1 (cm.)	R_2 (cm.)	H_1 (cm.)	H_2 (cm.)	W_1 (cm.)	W_2 (cm.)	T_a (°C.)	P_b (cm. Hg)
1	Th	-0.42	0.36	-0.92	0.75	13.82	11.58	28.9	73.21
2	Th	-1.60	1.52	-3.51	3.22	16.49	8.57	29.2	73.21
3	Th	-3.18	3.21	-6.59	6.24	20.47	4.59	29.1	73.21
4	Th	-4.72	4.80	-9.98	9.41	13.12*	11.31*	29.0	73.21
5	Th	-6.19	6.31	-13.11	12.43	13.38*	11.00*	29.0	73.21
6	Th	-7.52	7.70	-16.18	15.30	13.70*	10.78*	29.0	73.21
7	Th	-8.72	8.94	-18.82	17.81	13.90*	10.53*	29.0	73.21
Pressed to 300 lbs. ; L = 2.275 cm. ; V_t = 11.53 cm.^{3} ; ϵ = 0.706									
8	Th	-0.62	0.38	-1.02	0.74	13.30	11.12	26.3	73.08
9	Th	-1.37	1.18	-2.47	2.16	15.12	9.33	26.5	73.08
10	Th	-3.49	2.38	-6.75	6.31	20.49	4.00	26.5	73.08
11	Th	-5.00	4.91	-9.73	9.12	24.38	0.72	26.9	73.08
12	Th	-5.29	5.10	-10.21	9.39	13.10*	11.30*	26.9	73.08
13	Th	-7.56	7.50	-14.72	13.32	13.60*	10.90*	27.0	73.08
14	Th	-9.31	9.35	-18.18	17.08	13.90*	10.60*	27.0	73.08
Pressed to 500 lbs. ; L = 2.23 cm. ; V_t = 11.30 cm.^{3} ; ϵ = 0.699									
15	Th	-1.05	0.80	-2.00	1.63	14.19	10.13	27.1	73.22
16	Th	-2.30	2.15	-4.58	4.12	17.69	7.12	27.2	73.22
17	Th	-4.20	4.20	-8.65	8.08	22.87	2.10	27.3	73.22
18	Th	-6.06	6.03	-12.50	11.71	13.40*	11.10*	27.3	73.22
19	Th	-8.91	8.98	-18.50	17.38	13.91*	10.60*	27.4	73.22
20	/--/	-8.03	8.12	-2.80	2.51	21.20	3.51	29.3	73.58
21	/--/	-9.89	10.03	-3.46	3.14	23.27	1.50	29.4	73.58
22	/--/	-12.17	12.43	-4.22	3.91	13.28*	11.20*	29.4	73.58
23	/--/	-15.62	15.92	-5.50	5.11	13.50*	10.90*	29.3	73.58
24	/--/	-17.60	17.90	-6.19	5.81	13.70*	10.72*	29.9	73.58

* mercury manometer. Other "W" readings are with a water manometer.

Table 4. Experimental Data, WHRM-1 Kaolin Sample

d_s = 2.58 gm./cm.^{3}

w_s = 10.1990 gm. ; V_s = 3.96 cm.^{3}

Pressed to 100 lbs. ; L = 2.47 cm. ; V_t = 12.51 cm.^{3} ; ϵ = 0.683

Run	Cap.	R_1 (cm.)	R_2 (cm.)	H_1 (cm.)	H_2 (cm.)	W_1 (cm.)	W_2 (cm.)	T_a (°C.)	P_b (cm. Hg)
1	Th	26.89	27.37	23.16	23.79	30.56	28.76	28.3	74.44
2	Th	25.70	28.60	21.78	25.68	32.24	27.12	29.0	74.49
3	Th	24.63	29.73	20.50	26.40	34.11	25.25	29.1	74.49
4	Th	22.24	32.20	17.55	29.20	38.51	20.86	29.0	74.49
5	Th	20.09	34.41	14.74	31.89	22.43*	20.48*	29.0	74.51
6	Th	17.02	37.58	10.96	35.43	22.82*	20.06*	29.0	74.51
7	Th	14.88	39.73	8.74	38.05	23.09*	19.78*	29.0	74.51
8	Th	11.85	42.75	4.45	41.70	23.50*	19.86*	29.0	74.53
9	/--/	13.02	41.50	20.55	26.20	22.50*	20.39*	28.8	74.53
10	/--/	5.91	48.29	19.14	27.60	23.01*	19.89*	28.8	74.53
Pressed to 300 lbs. ; L = 2.26 cm. ; V_t = 11.47 cm.^{3} ; ϵ = 0.656									
11	Th	26.67	27.53	23.33	23.65	30.02	29.19	28.8	74.60
12	Th	25.25	28.98	21.94	24.98	32.46	26.77	29.0	74.65
13	Th	22.63	31.75	19.16	27.68	36.96	22.26	29.2	74.65
14	Th	19.18	35.94	15.59	31.18	22.43*	20.45*	29.2	74.65
15	Th	11.81	42.93	8.06	38.27	23.29*	19.56*	29.0	74.52
16	Th	7.88	46.68	4.11	42.13	23.77*	19.07*	29.0	74.57
17	Th	26.97	27.34	23.26	23.71	29.93	29.24	30.0	74.57

* mercury manometer. Other "W" readings are with a water manometer.

Table 5. Experimental Data, WHBM-1 Kaolin Sample

d_s = 2.58 gm./cm.^{3}

w_s = 9.2093 gm. ; V_s = 3.57 cm.^{3}

Pressed to 100 lbs. ; L = 2.26 cm. ; V_t = 11.43 cm.^{3} ; ϵ = 0.687

Run	Cap.	R_1 (cm.)	R_2 (cm.)	H_1 (cm.)	H_2 (cm.)	W_1 (cm.)	W_2 (cm.)	T_a (°C.)	P_b (cm. Hg)
1	Th	25.93	28.42	21.75	25.21	31.99	27.17	32.5	74.49
2	Th	24.57	29.87	19.83	27.09	34.71	24.47	33.0	74.45
3	Th	21.68	32.81	15.68	31.08	40.55	18.67	32.8	74.45
4	Th	18.72	35.90	11.25	35.26	22.68*	20.14	32.6	74.43
5	Th	26.85	27.42	23.17	23.82	29.99	29.08	31.3	74.30
6	Th	15.09	39.46	5.76	40.42	23.19*	19.61*	31.0	74.28
7	/--/	16.92	37.57	20.99	25.79	22.20*	20.62*	31.0	74.28
8	/--/	11.86	42.80	19.83	27.01	22.58*	20.34*	32.0	74.11
9	/--/	6.35	47.95	18.48	28.28	22.92*	19.85*	31.8	74.11
10	/--/	19.87	34.50	21.76	25.09	36.85*	22.22	30.6	73.95
Pressed to 300 lbs. ; L = 2.15 cm. ; V_t = 10.90 cm.^{3} ; ϵ = 0.671									
11	Th	26.68	27.50	22.66	24.19	30.45	28.55	30.2	73.97
12	Th	24.43	29.76	20.12	26.61	34.24	24.77	29.7	73.97
13	Th	20.19	34.12	14.63	31.89	22.33*	20.42*	29.7	73.94
14	Th	13.12	41.44	5.33	40.77	23.33*	19.47*	31.0	73.90

* mercury manometer. Other "W" readings are with a water manometer.

Table 6. Experimental Data, WHBM-24 Kaolin Sample

d_s = 2.58 gm./cm.^{3}

w_s = 9.7643 gm. ; V_s = 3.79 cm.^{3}

Pressed to 100 lbs. ; L = 2.06 cm. ; V_t = 10.47 cm.^{3} ; ϵ = 0.639

Run	Cap.	R_1 (cm.)	R_2 (cm.)	H_1 (cm.)	H_2 (cm.)	W_1 (cm.)	W_2 (cm.)	T_a (°C.)	P_b (cm. Hg)
1	Th	25.83	28.32	22.66	24.15	31.04	27.80	29.8	73.90
2	Th	24.23	29.96	21.67	25.11	33.08	25.75	29.8	73.90
3	Th	22.73	32.97	20.28	26.93	37.00	22.24	29.9	73.83
4	Th	16.48	38.38	16.95	30.14	22.60*	20.44*	29.9	73.82
5	Th	12.39	42.55	14.48	32.58	23.00*	20.04*	29.9	73.80
6	Th	7.37	47.29	11.28	35.58	23.48*	19.56*	29.9	73.78

* mercury manometer. Other "W" readings are with a water manometer.

Table 7. Experimental Data, ASTM Kaolin Sample

d_s = 2.58 gm./cm.^{3}

w_s = 14.0919 gm. ; V_s = 5.455 cm.^{3}

Pressed to 100 lbs. ; L = 2.675 cm. V_t = 13.58 cm.^{3} ; ϵ = 0.599

Run	Cap.	R_1 (cm.)	R_2 (cm.)	H_1 (cm.)	H_2 (cm.)	W_1 (cm.)	W_2 (cm.)	T_a (°C.)	P_b (cm. Hg)
1	Th	26.15	28.53	22.33	25.06	31.69	27.49	30.8	73.39
2	Th	27.03	27.59	23.35	24.05	30.09	29.09	30.8	73.39
3	Th	25.59	29.10	21.55	25.80	32.69	26.50	31.0	73.37
4	Th	22.36	32.41	17.58	29.61	38.59	20.60	30.4	73.37
5	Th	16.29	38.68	9.62	37.15	23.05*	20.00*	30.6	73.36
6	Th	11.73	43.26	3.73	42.76	23.65*	19.39*	30.3	73.36

* mercury manometer. Other "W" readings are with a water manometer.

Table 8. Experimental Data, 1556-AB Al_2O_3 Grinding Powder

d_s = 4.00 gm./cm.^{3}

w_s = 20.2020 gm. ; V_s = 5.05 cm.^{3}

Pressed to 100 lbs. ; L = 3.50 cm. ; V_t = 17.71 cm.^{3} ; ϵ = 0.715

Run	Cap.	R_1 (cm.)	R_2 (cm.)	H_1 (cm.)	H_2 (cm.)	W_1 (cm.)	W_2 (cm.)	T_a (°C.)	P_b (cm. Hg)
1	Th	27.15	27.65	23.36	24.14	30.20	29.28	31.2	73.40
2	Th	26.28	28.47	21.91	25.56	32.10	27.38	32.0	73.40
3	Th	25.07	29.83	19.81	27.65	35.00	24.50	33.0	73.30
4	Th	22.86	32.12	15.88	31.39	22.33*	20.81*	32.4	73.30
5	Th	16.06	39.06	4.09	42.60	23.41*	19.72*	33.0	73.32
6	/--/	15.84	38.91	22.55	28.89	22.49*	20.67*	32.0	73.32
7	/--/	9.81	45.11	19.92	29.76	22.94*	20.20*	31.8	73.38
8	/--/	18.92	35.89	23.56	28.24	38.68	21.02	31.0	73.38

* mercury manometer. Other "W" readings are with a water manometer.

Table 9. Experimental Data, 1560-S-AB Emery Grinding Compound

d_s = 3.55 gm./cm.^{3}

w_s = 19.4019 gm. ; V_s = 5.46 cm.^{3}

Pressed to 100 lbs. ; L = 2.445 cm. ; V_t = 12.39 cm.^{3} ; ϵ = 0.560

Run	Cap.	R_1 (cm.)	R_2 (cm.)	H_1 (cm.)	H_2 (cm.)	W_1 (cm.)	W_2 (cm.)	T_a (°C.)	P_b (cm.Hg)
1	/--/	26.68	27.92	23.64	28.23	32.18	27.43	31.6	73.40
2	/--/	25.55	29.11	19.20	32.48	36.70	22.98	31.2	73.40
3	/--/	24.25	30.46	13.90	37.58	22.50*	20.65*	31.2	73.40
4	/--/	22.90	31.87	7.78	43.32	22.90*	20.21*	31.1	73.40
5	11	19.91	34.91	24.90	27.09	22.10*	21.04*	31.1	73.40
6	11	15.70	39.26	24.27	27.72	22.41*	20.74*	31.0	73.40
7	11	8.07	46.73	23.11	28.86	22.91*	20.21*	31.2	73.40

* mercury manometer. Other "W" readings are with a water manometer.

Table 10. Experimental Data, 1561-AB Emery Grinding Compound

d_s = 3.55 gm./cm.^{3}

w_s = 20.1734 gm. ; V_s = 5.68 cm.^{3}

Pressed to 100 lbs. ; L = 2.38 cm. ; V_t = 12.08 cm.^{3} ; ϵ = 0.530

Run	Cap.	R_1 (cm.)	R_2 (cm.)	H_1 (cm.)	H_2 (cm.)	W_1 (cm.)	W_2 (cm.)	T_a (°C.)	P_b (cm. Hg)
1	Th	27.00	27.78	25.48	26.78	30.57	28.91	33.0	73.26
2	Th	27.03	27.75	25.50	26.76	30.57	28.91	33.0	73.26
3	Th	23.68	31.10	19.21	32.26	37.87	21.64	33.1	73.26
4	Th	19.40	35.63	11.08	40.41	22.93*	20.17*	33.2	73.26
5	/--/	15.96	39.05	25.27	26.86	22.32*	20.30*	33.2	73.26
6	/--/	10.83	44.26	24.93	27.24	22.66*	20.47*	33.2	73.26
7	/--/	7.30	47.50	24.68	27.49	22.87*	20.28*	33.3	73.26

* mercury manometer. Other "W" readings are with a water manometer.

APPENDIX E

SAMPLE CALCULATIONS

Density of Emery Grinding Compound

Pycnometer Volume = 10.00 $cm.^3$

Empty Weight = 16.3103 gm.

wt. of pycmometer + 10.00 $cm.^3$ deaereated

n butyl phthalate = 26.6360 gm.

less 16.3103 gm.

10.3257 gm. n butyl phthalate per 10.00 $cm.^3$

1561 AB Emery Grinding Compound:

wt. of pycnometer + powder = 20.4631 gm.

less 16.3103 gm.

4.1528 grams of sample.

wt. of pycnometer + powder + n butyl phthalate

= 29.5799 gm.

less 20.4631 gm.

9.1168 gm. of n phthalate

Therefore the volume occupied by the n butyl phthalate is

$$\frac{9.1168 \text{ gm.}}{1.03257 \text{ gm./cm.}^3} = 8.8293 \text{ cm.}^3$$

Therefore the 4.1528 gm. of powder occupied 10.000 - 8.8293 = 1.1707 $cm.^3$

Therefore

$$d_s = \frac{4.1528 \text{ gm.}}{1.1707 \text{ cm.}^3} = 3.55 \text{ gm./cm.}^3 \text{ for the emery grinding compound}$$

The Lea and Nurse Equation

Equation (14) is the Lea and Nurse equation.

$$S_w = \frac{14}{d(1-\epsilon)}\sqrt{\frac{\epsilon^3 A h_1}{C L h_2}} \qquad (14)$$

From equation (11),

$$C = \frac{Q\mu}{h_2 d_m}$$

Calculation of Capillary Constants:

CROSS-CALIBRATION DATA FOR THERMOMETER CAPILLARY AND /--/ CAPILLARY

$\frac{Q}{\text{L.(s.t.p.)}/\text{hr.}}$	Thermom. h_2 (cm.)	/--/ h_2 (cm.)	$\frac{Q}{(\text{cm.}^3/\text{sec.})}$	Thermom. $Q/h_2 \times 10^4$ $(\text{cm.}^2/\text{sec.})$	/--/ $Q/h_2 \times 10^3$ $(\text{cm.}^2/\text{sec.})$
0.01918	7.05	1.4	0.00530	7.52	4.65
0.0423	14.87	2.44	0.01174	7.90	4.81
0.0630	22.27	3.62	0.01750	7.96	4.84
0.0883	31.00	5.01	0.0245	7.90	4.89
0.1127	38.96	6.29	0.0313	8.04	4.99
0.0480	16.90	2.82	0.01332	7.89	4.73
0.0224	7.92	1.33	0.00622	7.85	4.68
0.0689	23.69	4.02	0.01911	8.08	4.75
0.1186	39.81	6.88	0.0329	8.26	4.79

d_m = 0.827 gm./cm.^{3} ; μ = 1.832x10^{-4} poise; μ/d_m = 2.22x10^{-4}

Thermometer capillary:

$$(Q/h_2)_{Ave.} = 0.000792$$

$$C = 1.76\text{x}10^{-7} \text{ cm.}^4/\text{sec.}^2$$

/--/ capillary:

$$(A/h_2)_{Ave.} = 0.00479$$

$$C = 1.062\text{x}10^{-6} \text{ cm.}^4/\text{sec.}^2$$

Constant, C, for Capillary No. 11:

$\frac{Q}{\text{(L.(s.t.p.)/hr.)}}$	$\frac{h_2}{\text{(cm.)}}$	$\frac{Q}{\text{(cm.}^3\text{/sec.)}}$	$\frac{Q/h_2}{\text{(cm.}^2\text{/sec.)}}$
0.569	1.07	0.158	0.1478
0.745	1.41	0.207	0.1469
2.140	4.26	0.595	0.1393
7.12	15.98	1.98	0.1240
11.94	26.23	3.32	0.1265

Capillary No. 11:

$$(Q/h_2)_{Ave.} = 0.1369$$

$$C = 3.04\text{x}10^{-5} \text{ cm.}^4/\text{sec.}^2$$

Surface area calculation by equation (14):

WH Kaolin Sample.

$\epsilon = 0.719$; $L = 2.385$ cm.; $d = 2.58$ gm./cm.^{3}; $A = 5.067$ cm.^{2}

$$S_w = \frac{14}{d(1-\epsilon)}\sqrt{\frac{\epsilon^3 A h_1}{C L h_2}} = \frac{14}{(2.58)(0.281)}\sqrt{\frac{(0.719)^3(5.067)}{(1.76\times10^{-7})(2.385)}}\sqrt{\frac{h_1}{h_2}}$$

$$S_w = 4.08 \times 10^4\sqrt{\frac{h_1}{h_2}} \quad \text{cm.}^2/\text{gm.}$$

h_1 (cm.)	h_2 (cm.)	h_1/h_2	$\sqrt{h_1/h_2}$	S_w (m.^{2}/gm.)
0.78	1.67	0.466	0.683	2.78
3.12	6.37	0.490	0.700	2.86
6.39	12.83	0.497	0.705	2.88
9.52	19.39	0.491	0.701	2.86
12.10	25.44	0.474	0.698	2.80
15.22	31.48	0.484	0.695	2.84
17.66	36.63	0.481	0.694	2.83

$$(S_w)_{Ave.} = 2.83 \quad \text{m.}^2/\text{gm.}$$

The Lyon Equation

Equation (36) is the Lyon equation in terms of S_w.

$$F = \frac{QP_1}{\Delta P} = \frac{A\epsilon^3}{\mu kLd^2 S_w(1-\epsilon)^2} \cdot \bar{P} + \frac{8}{3}\sqrt{\frac{2RT}{\pi M}} \cdot \frac{A}{LdS_w} \cdot \frac{\epsilon^3}{(1-\epsilon)} \qquad (36)$$

a plot of F vs. $\bar{P}$ has for a slope, $\frac{A\epsilon^3}{\mu kLd^2 S_w(1-\epsilon)^2}$,

and an intercept of $\frac{8}{3}\sqrt{\frac{2RT}{\pi M}} \cdot \frac{A}{LdS_w} \cdot \frac{\epsilon^3}{(1-\epsilon)}$.

None of the data treated had a positive slope, and so all of the data was assumed to have a zero slope. The values of F near $\bar{P} = P_b$ were consistently low and hence neglected in averaging the other values of F to determine the mean value for the intercept.

For a zero slope, equation (36) becomes,

$$F = \frac{QPq}{\Delta P} = \frac{8}{3}\sqrt{\frac{2RT}{\pi M}} \cdot \frac{A^2}{LdS_w} \cdot \frac{\epsilon^3}{(1-\epsilon)} \cdot$$

Substituting, $R = 8.3156 \times 10^7 \frac{\text{ergs.}}{\text{mole } {}^{o}\text{K.}}$

$M = 29$ gm./gm. mole

$A = 5.067$ cm.^{2}

$$F = 1.822 \times 10^4 \frac{\epsilon^3 \sqrt{T}}{LdS_w (1-\epsilon)}$$

The following is a sample calculation for Run (1) with the WH Kaolin Sample for $\epsilon = 0.719$.

Experimental data:

$h_1 = 0.78$ cm. red oil, $d_m = 0.827$ gm./cm.^{3}

$h_2 = 1.67$ cm. red oil, using the thermometer capillary.

$h_3 = 2.24$ cm. H_2O

$T = 302.1^{o}K$

$P_b = 73.21$ cm. Hg

$L = 2.385$ cm.

$d = 2.58$ gm./cm.^{3}

ΔP across the bed $= 0.78$ cm. red oil $\frac{(0.827 \text{ gm./cm.}^3)}{(13.52 \text{ gm./cm.}^3 \text{Hg})} = 0.0477$ cm. Hg

Vacuum in surge bottle = 2.24 cm. H_2O $\frac{(0.996 \text{ gm./cm.}^3)}{(13.52 \text{ gm./cm.}^3 \text{Hg.})}$ = 0.165 cm. Hg.

$$P_1 = 73.21 - 0.05 = 73.16 \text{ cm. Hg.}$$

$$P_2 = 73.21 - 0.17 = 0.17 = 73.04 \text{ cm. Hg.}$$

$$\bar{P}' = \frac{P_b + P_1}{2} = \frac{73.21 + 73.16}{2} = 73.18 \text{ cm. Hg.}$$

From Figure 16 at h_2 = 1.67, L.(s.t.p.)/hr = 0.00437

$$Q = (0.00437 \text{ L./hr.})\left(\frac{1000 \text{ cm.}^3/\text{L.}}{3600 \text{ sec./hr.}}\right) = 0.001214$$

$$\frac{P_q}{\bar{P}} = \frac{76.00}{0.0477} = 1591$$

$$F = \frac{QP_q}{\bar{P}} = 1.932$$

Calculation of S_w:

From Figure 6, $F_{Ave.}$ = 1.991, slope = 0

$$F = 1.822 \times 10^4 \frac{\epsilon^3 \sqrt{T}}{LdS_w(1-\epsilon)}$$

$$1.991 = \frac{1.822 \times 10^4 (0.719)^3 \ 302.1}{(2.385)(2.58) \ S_w \ (0.281)}$$

or $S_w = 3.41 \times 10^4$ cm.^{2}/gm., which is equivalent to

$$S_w = 3.41 \text{ m.}^2/\text{gm.}$$

The Fanning Friction Factor-Reynolds Number Relation

Equation (48) expresses the Fanning friction factor-Reynolds number relation.

$$\frac{\Delta h g D_c}{2u^2 L} = f = \left[\frac{D_c u d}{\mu} \cdot \frac{\epsilon^3}{(1-\epsilon)^2}\right] = \phi N_{Re} \quad . \tag{48}$$

For purposes of calculation f was expressed as,

$$f = - \frac{\Delta P x 980.597)\ D_c}{2du^2 L}$$

if Δ P is in gm./cm.^{2}, then (Δ Px980.597) is in dynes/cm.^{2}

$D_c = \frac{4\epsilon}{(1-\epsilon)dS_w}$, and for the data given in Figure 14

S_w was taken from the Lyon equation in cm.^{2}/gm.

Δ P is negative, therefore f is positive.

$$f = \frac{(\text{dynes/cm.}^2)(\text{cm.})}{(\text{gm./cm.}^3)(\text{cm.}^2/\text{sec.}^2)(\text{cm.})}$$

$$f = \frac{(\text{gm.-cm./sec.}^2\text{-cm.}^2)(\text{cm.})}{(\text{gm./sec.}^2)} = \text{dimensionless.}$$

$$N_{Re} = \frac{(\text{cm.})(\text{cm./sec.})(\text{gm./cm.}^3)}{(\text{poise})}$$

$$N_{Re} = \frac{(\text{gm./cm.-sec.})}{(\text{gm./cm.-sec.})} = \text{dimensionless}$$

Calculation for WH Clay Sample. ϵ = 0.719, L = 239 cm.:

From the Lyon equation, $S_w = 3.41 \times 10^4$ cm.^{2}/gm.

$$D_c = \frac{4\epsilon}{(1-\epsilon)dS_w} = \frac{4(0.719)}{(0.281)(2.58)(3.41 \times 10^4)} = 1.167 \times 10^4 \text{ cm.}$$

$\mu = 1.834 \times 10^{-4}$ poise

$$u = \frac{Q}{A} = \frac{Q_{s.t.p.}}{5.067} \left(\frac{302}{273}\right) \left(\frac{760}{732}\right) = 0.2265\ Q_{s.t.p.}$$

$$f = \frac{\Delta P D_c}{2u^2 L d} \quad \frac{(\Delta P' x 980)(1.167x10^{-4}}{2(u^2 x10^6)(dx10^3)(10^{-6})(10^{-3})(2.39)}$$

$$f = 2.39x10^7 \quad \frac{\Delta P'}{(u^2 x10^6)(dx10^3)}$$

$$N_{Re} = \frac{D_c ud}{\mu} \cdot \frac{\epsilon^3}{(1-\epsilon)^2}$$

$$N_{Re} = \frac{(1.167x10^{-4})(ux10^3)(10^{-3})(dx10^3)(10^{-3})(0.719)^3}{(1.834x10^{-4})(0.281)^2}$$

$$N_{Re} = 2.98x10^{-6} \quad (ux10^3)(dx10^3)$$

Run	$u\ x10^3$ (cm./sec.)	$u^2 x10^6$ $(cm./sec.)^2$	f	N_{Re}
1	0.2755	0.0759	$1.816x10^8$	$9.26x10^{-7}$
2	1.161	1.350	$4.08x10^7$	$3.90x10^{-6}$
3	2.255	5.09	$2.22x10^7$	$7.55x10^{-6}$
4	3.48	12.10	$1.388x10^7$	$1.168x10^{-5}$
5	4.455	19.85	$1.118x10^7$	$1.492x10^{-5}$
6	5.695	32.40	$8.31x10^6$	$1.900x10^{-5}$
7	6.55	42.95	$7.30x10^6$	$2.182x10^{-5}$

Reduction to nitrogen adsorption surface area value:

From equation (49) it is seen that

$$f = \frac{\Delta h \quad g \quad 4\epsilon}{2u^2(1-\epsilon)d_s} \cdot \frac{1}{S_w} = K\frac{1}{S_w} \ ,$$

and $$N_{Re} = \left\{ \frac{4 \epsilon^4 ud}{(1-\epsilon)^3 \mu d_s} \right\} \frac{1}{S_w} = K' \cdot \frac{1}{S_w} \quad .$$

Therefore,

$$\frac{n_f}{l_f} = \frac{l_{S_w}}{n_{S_w}} \, ,$$

where

n_f = the Fanning friction factor based on the nitrogen adsorption value for the surface area,

l_f = the Fanning friction factor based on the value of surface area calculated using the Lyon equation,

l_{S_w} = the surface area per unit weight calculated by using the Lyon equation, and

n_{S_w} = the surface area per unit weight determined by nitrogen adsorption.

Similarly,

$$\frac{n_{N_{Re}}}{l_{N_{Re}}} = \frac{l_{S_w}}{n_{S_w}} \, , \text{ or } n_{N_{Re}} \cdot \frac{l_{S_w}}{n_{S_w}} \quad .$$

For the WH Kaolin Sample,

$$l_{S_w} = 3.40 \times 10^4 \, ,$$

and $$n_{S_w} = 7.60 \times 10^4 \quad .$$

Therefore

$$n_f = \frac{3.40 \times 10^4}{7.60 \times 10^4} \cdot {}^1f = 0.448 \, {}^1f \ ,$$

and, $$n_{N_{Re}} = 0.448 \, {}^1N_{Re} \ .$$

Therefore, for Run 1,

$$n_f = 8.11 \times 10^7 \ ,$$

and $$n_{N_{Re}} = 4.15 \times 10^{-7} \ .$$

The Equation of the Reduced Line

Figure 15 shows the reduced line to have a negative slope of 1.0. Therefore,

$$\log f = - \log N_{Re} + \log b \ ,$$

or

$$f = \frac{b}{N_{Re}} \ .$$

Therefore,

$$b = f \, N_{Re} \ .$$

By multiplying f by N_{Re} for all the runs made with the WH, WHRM-1 WHBM-1, and WHBM-24 Kaolin samples and taking an average, b was determined to be 21.9. Therefore the equation of the reduced line is

$$f = \frac{21.9}{N_{Re}} \ .$$

Calculation of Surface Area Using the Reduced Line

Refer to Figure 15, and the ASTM Kaolin Sample line. The surface area value used to construct this line was calculated from the Lyon equation.

Trial (1) $$\frac{f_q}{f_j} = \frac{4.0 \times 10^8}{2.14 \times 10^8} = 1.869$$

$$\frac{(N_{Re})_q}{(N_{Re})_d} = \frac{1.93 \times 10^{-7}}{1.03 \times 10^{-7}} = 1.871$$

Trial (2) $$\frac{f_q}{f_j} = \frac{2.90 \times 10^7}{1.55 \times 10^7} = 1.870$$

$$\frac{(N_{Re})_q}{(N_{Re})_d} = \frac{2.60 \times 10^7}{1.39 \times 10^7} = 1.870$$

Average correction factor = 1.870

Therefore:

$$S_w = 1.87 \times 2.00 = 3.74 \times 10^4 \text{ cm.}^2/\text{gm.}$$

APPENDIX F

CALCULATED DATA

Table 11. Calculated Data, WH Kaolin Sample

Run	F ($cm.^3/sec.$)	$\overline{P}$ (cm.Hg)	Data for Fig. 14 Basis, Lyon S_w f	Data for Fig. 14 Basis, Lyon S_w N_{Re}	Data for Fig. 15 Basis, B.E.T. S_w f	Data for Fig. 15 Basis, B.E.T. S_w N_{Re}
ϵ = 0.719						
1	1.932	73.18	1.816×10^{8}	9.26×10^{-7}	8.11×10^{7}	4.15×10^{-7}
2	2.040	73.11	4.08×10^{7}	3.90×10^{-6}	1.825×10^{7}	1.744×10^{-6}
3	1.939	73.01	2.22×10^{7}	7.55×10^{-6}	9.94×10^{6}	3.38×10^{-6}
4	2.002	72.92	1.388×10^{7}	1.168×10^{-5}	6.20×10^{6}	5.22×10^{-6}
5	1.952	72.82	1.118×10^{7}	1.492×10^{-5}	5.00×10^{6}	6.69×10^{-6}
6	2.042	72.74	8.31×10^{6}	1.900×10^{-5}	3.72×10^{6}	8.50×10^{-6}
7	2.032	72.67	7.30×10^{6}	2.182×10^{-5}	3.26×10^{6}	9.76×10^{-6}
ϵ = 0.706						
8	1.598	73.06	1.968×10^{8}	7.64×10^{-7}	9.20×10^{7}	3.58×10^{-7}
9	1.713	73.00	6.66×10^{7}	2.09×10^{-6}	3.12×10^{7}	9.79×10^{-7}
10	2.110	72.90	1.930×10^{7}	5.90×10^{-6}	9.01×10^{6}	2.76×10^{-6}
11	1.884	72.77	1.431×10^{7}	8.85×10^{-6}	6.70×10^{6}	4.15×10^{-6}
12	1.860	72.76	1.405×10^{7}	9.15×10^{-6}	6.58×10^{6}	4.29×10^{-6}
13	1.849	72.62	9.80×10^{6}	1.270×10^{-5}	4.59×10^{6}	5.95×10^{-6}
14	1.922	72.51	7.69×10^{6}	1.660×10^{-5}	3.60×10^{6}	7.76×10^{-6}
ϵ = 0.699						
15	1.842	73.16	8.85×10^{7}	1.606×10^{-6}	3.67×10^{7}	6.65×10^{-7}
16	1.890	73.08	3.49×10^{7}	3.96×10^{-6}	1.448×10^{7}	1.641×10^{-6}
17	1.932	72.96	1.756×10^{7}	7.70×10^{-6}	7.28×10^{6}	3.19×10^{-6}
18	1.981	72.85	1.178×10^{7}	1.121×10^{-5}	4.88×10^{6}	4.65×10^{-6}

Table 11. Calculated Data, WH Kaolin Sample (Concl.)

Run	F ($cm.^3/sec.$)	$\bar{P}$ (cm. Hg)	Data for Fig. 14 Basis, Lyon S_w f	Data for Fig. 14 Basis, Lyon S_w N_{Re}	Data for Fig. 15 Basis, B.E.T. S_w f	Data for Fig. 15 Basis, B.E.T. S_w N_{Re}
ϵ = 0.699						
19	1.991	72.67	7.95×10^{6}	1.661×10^{-5}	3.295×10^{6}	6.89×10^{-6}
20	1.990	73.08	8.79×10^{6}	1.500×10^{-5}	3.64×10^{6}	6.21×10^{-6}
21	2.195	72.97	6.85×10^{6}	1.879×10^{-5}	2.84×10^{6}	7.79×10^{-6}
22	2.000	72.82	5.75×10^{6}	2.28×10^{-5}	2.38×10^{6}	9.45×10^{-6}
23	2.060	72.61	4.20×10^{6}	3.01×10^{-5}	1.74×10^{6}	1.248×10^{-5}
24	2.070	72.37	3.69×10^{6}	3.41×10^{-5}	1.530×10^{6}	1.412×10^{-5}

Table 12. Calculated Data, WHRM-1 Kaolin Sample

Run	F ($cm.^3/sec.$)	$\bar{P}$ (cm. Hg)	Data for Fig. 14 Basis, Lyon S_w f	Data for Fig. 14 Basis, Lyon S_w N_{Re}	Data for Fig. 15 Basis, B.E.T. S_w f	Data for Fig. 15 Basis, B.E.T. S_w N_{Re}
ϵ = 0.683						
1	0.979	74.42	5.77×10^{8}	1.550×10^{-7}	2.52×10^{8}	6.75×10^{-8}
2	1.242	74.40	7.81×10^{7}	1.073×10^{-6}	3.41×10^{7}	4.69×10^{-7}
3	1.087	74.33	5.65×10^{7}	1.610×10^{-6}	2.46×10^{7}	7.03×10^{-7}
4	1.139	74.18	2.90×10^{7}	3.14×10^{-6}	1.265×10^{7}	1.370×10^{-6}
5	1.188	74.07	1.780×10^{7}	4.81×10^{-6}	7.76×10^{6}	2.10×10^{-6}
6	1.190	73.88	1.242×10^{7}	6.86×10^{-6}	5.42×10^{6}	2.995×10^{-6}
7	1.180	73.75	1.041×10^{7}	8.24×10^{-6}	4.55×10^{6}	3.59×10^{-6}
8	1.201	73.58	8.09×10^{6}	1.041×10^{-5}	3.525×10^{6}	4.55×10^{-6}
9	1.210	73.66	8.65×10^{6}	9.67×10^{-6}	3.77×10^{6}	4.21×10^{-6}
10	1.220	73.23	5.76×10^{6}	1.440×10^{-5}	2.515×10^{6}	6.29×10^{-6}

Table 12. Calculated Data, WHRM-1 Kaolin Sample (Concl.)

Run	F ($cm.^3/sec.$)	$\bar{P}$ (cm. Hg)	Data for Fig. 14 Basis, Lyon S_w f	Data for Fig. 14 Basis, Lyon S_w N_{Re}	Data for Fig. 15 Basis, B.E.T. S_w f	Data for Fig. 15 Basis, B.E.T. S_w N_{Re}
ϵ = 0.656						
11	0.311	74.57	3.61×10^{9}	6.15×10^{-8}	1.810×10^{9}	2.08×10^{-8}
12	0.769	74.54	1.809×10^{8}	6.56×10^{-7}	9.05×10^{7}	3.29×10^{-7}
13	0.907	74.37	5.15×10^{7}	1.905×10^{-6}	2.58×10^{7}	9.54×10^{-7}
14	0.915	74.13	2.17×10^{7}	3.49×10^{-6}	1.088×10^{7}	1.749×10^{-6}
15	0.950	73.57	1.389×10^{7}	6.65×10^{-6}	6.95×10^{6}	3.33×10^{-6}
16	0.951	73.38	8.81×10^{7}	8.27×10^{-6}	4.41×10^{7}	4.15×10^{-6}
17	0.949	74.51	3.02×10^{8}	7.97×10^{-7}	1.512×10^{8}	4.00×10^{-7}

Table 13. Calculated Data, WHBM-1 Kaolin Sample

Run	F ($cm.^3/sec.$)	$\bar{P}$ (cm. Hg)	Data for Fig. 14 Basis, Lyon S_w f	Data for Fig. 14 Basis, Lyon S_w N_{Re}	Data for Fig. 15 Basis, B.E.T. S_w f	Data for Fig. 15 Basis, B.E.T. S_w N_{Re}
ϵ = 0.687						
1	1.305	74.41	9.81×10^{7}	1.002×10^{-6}	4.46×10^{7}	4.56×10^{-7}
2	1.300	74.29	4.63×10^{7}	2.13×10^{-6}	2.10×10^{7}	9.70×10^{-7}
3	1.350	74.11	2.60×10^{7}	4.63×10^{-6}	1.182×10^{7}	2.10×10^{-6}
4	1.381	73.90	1.275×10^{7}	7.30×10^{-6}	5.80×10^{6}	3.32×10^{-6}
5	0.981	74.28	7.56×10^{8}	1.738×10^{-7}	3.44×10^{8}	7.90×10^{-8}
6	1.410	73.48	8.65×10^{6}	1.053×10^{-5}	3.94×10^{6}	4.80×10^{-6}
7	1.398	73.65	1.038×10^{7}	8.85×10^{-6}	4.71×10^{6}	4.03×10^{-6}
8	1.390	73.16	7.03×10^{6}	1.311×10^{-5}	3.20×10^{6}	5.97×10^{-6}
9	1.409	72.83	5.10×10^{6}	1.780×10^{-5}	2.32×10^{6}	8.10×10^{-6}
10	1.343	73.50	1.582×10^{7}	5.98×10^{-6}	7.20×10^{6}	2.72×10^{-6}

Table 13. Calculated Data, WHBM-1 Kaolin Sample (Concl.)

Run	F ($cm.^3/sec.$)	$\bar{P}$ (cm. Hg)	Data for Fig. 14 Basis, Lyon S_w f	Data for Fig. 14 Basis, Lyon S_w N_{Re}	Data for Fig. 15 Basis, B.E.T. S_w f	Data for Fig. 15 Basis, B.E.T. S_w N_{Re}
ϵ = 0.671						
11	1.610	73.94	1.832×10^{8}	3.30×10^{-7}	8.76×10^{7}	1.577×10^{-7}
12	1.161	73.80	5.30×10^{7}	1.568×10^{-6}	2.53×10^{7}	7.50×10^{-7}
13	1.228	73.51	1.828×10^{7}	4.305×10^{-6}	8.74×10^{6}	2.06×10^{-6}
14	1.238	73.03	8.91×10^{6}	8.74×10^{-6}	4.26×10^{6}	4.18×10^{-6}

Table 14. Calculated Data, WHBM-24 Kaolin Sample

Run	F ($cm.^3/sec.$)	$\bar{P}$ (cm. Hg)	Data for Fig. 14 Basis, Lyon S_w f	Data for Fig. 14 Basis, Lyon S_w N_{Re}	Data for Fig. 15 Basis, B.E.T. S_w f	Data for Fig. 15 Basis, B.E.T. S_w N_{Re}
ϵ = 0.639						
1	0.540	73.82	2.70×10^{8}	1.120×10^{-7}	1.629×10^{8}	6.76×10^{-8}
2	0.559	73.72	1.092×10^{8}	2.66×10^{-7}	6.60×10^{7}	1.607×10^{-7}
3	0.609	73.51	5.17×10^{7}	5.16×10^{-7}	3.12×10^{7}	3.115×10^{-7}
4	0.5795	73.15	2.69×10^{7}	1.048×10^{-6}	1.621×10^{7}	6.33×10^{-7}
5	0.580	72.88	1.966×10^{7}	1.437×10^{-6}	1.202×10^{7}	8.66×10^{-7}
6	0.593	72.56	1.821×10^{7}	1.910×10^{-6}	1.100×10^{7}	1.052×10^{-6}

Table 15. Calculated Data, ASTM Kaolin Sample

ϵ	Run	F ($cm.^3/sec.$)	$\bar{P}$ (cm.Hg)	Data for Fig. 15 Basis, Lyon S_w f	N_{Re}
0.639	1	1.069	73.31	2.43×10^{8}	4.39×10^{-7}
	2	1.060	73.38	8.59×10^{8}	9.60×10^{-8}
	3	1.129	73.26	1.058×10^{8}	6.82×10^{-7}
	4	0.914	73.06	5.70×10^{7}	1.577×10^{-6}
	5	1.252	72.67	1.351×10^{7}	4.805×10^{-6}
	6	1.210	72.39	1.040×10^{7}	6.50×10^{-6}

Table 16. Calculated Data, 1556-AB Al_2O_3 Grinding Powder

ϵ	Run	F ($cm.^3/sec.$)	$\bar{P}$ (cm.Hg)	Data for Fig. 15 Basis, Lyon S_w f	N_{Re}
0.715	1	1.350	73.39	3.82×10^{8}	3.03×10^{-7}
	2	1.538	73.33	5.61×10^{7}	1.510×10^{-6}
	3	1.732	73.15	2.02×10^{7}	3.70×10^{-6}
	4	1.620	73.01	1.196×10^{7}	6.65×10^{-6}
	5	1.635	72.61	4.75×10^{6}	1.670×10^{-5}
	6	1.641	72.61	4.68×10^{6}	1.680×10^{-5}
	7	1.662	72.30	3.66×10^{6}	2.60×10^{-5}
	8	1.632	72.86	6.39×10^{6}	1.241×10^{-5}

Table 17. Calculated Data, 1560-S-AB Emery Grinding Compound

ϵ	Run	F ($cm.^3/sec.$)	$\bar{P}$ (cm.Hg)	Data for Fig. 15 Basis, Lyon S_w f	N_{Re}
0.560	1	22.25	73.36	1.780×10^{7}	6.95×10^{-5}
	2	23.30	73.29	5.65×10^{6}	1.675×10^{-4}
	3	24.20	73.21	2.99×10^{6}	3.035×10^{-4}
	4	25.60	73.13	1.875×10^{6}	4.61×10^{-4}
	5	25.50	72.94	1.126×10^{6}	9.75×10^{-4}
	6	25.20	72.68	7.40×10^{5}	1.210×10^{-3}
	7	25.02	72.22	4.61×10^{5}	1.979×10^{-3}

Table 18. Calculated Data, 1561-AB Emery Grinding Compound

ϵ	Run	F ($cm.^3/sec.$)	$\bar{P}$ (cm.Hg)	Data for Fig. 15 Basis, Lyon S_w f	N_{Re}
0.530	1	9.46	73.23	8.44×10^{7}	6.81×10^{-6}
	2	10.08	73.24	7.62×10^{7}	6.70×10^{-6}
	3	10.81	73.02	6.41×10^{6}	7.41×10^{-5}
	4	11.38	72.76	2.67×10^{6}	1.697×10^{-4}
	5	11.70	72.55	1.780×10^{6}	2.47×10^{-4}
	6	11.63	72.23	1.241×10^{6}	3.54×10^{-4}
	7	11.50	72.03	1.060×10^{6}	4.20×10^{-4}

VITA

VITA

Robert Allen McAllister was born on February 19, 1923 in Indianapolis, Indiana. He was graduated from Greensboro High School, Greensboro, North Carolina in June 1940, ranking fifth in a class of over 300.

His college career began at Guilford College, Guilford College, North Carolina, where he majored in chemistry. After completing his sophomore year at Guilford College, he transferred to the chemical engineering course at North Carolina State College in Raleigh, North Carolina. After one year at North Carolina State he was called to active duty in the U. S. Naval V-12 Program and assigned to the University of Virginia on July 1, 1943, continuing a chemical engineering major. Here he was made a member of Theta Tau Engineering Society. After one school year at the University of Virginia he was sent to the U. S. Naval Midshipmen's School, U. S. S. Prairie State, at Columbia University in New York, N.Y.

He was commissioned Ensign on October 26, 1944 and assigned to the U. S. S. YMS-176, a minesweeper, as engineering officer. The ship was in the Asiatic-Pacific Theater of Operations and took part in the Lingayen Gulf Invasion, the Okinawa Invasion, and the Occupation of Japan. Ensign McAllister was released from active duty on June 26, 1946.

He then returned to North Carolina State College where he

completed the Bachelor of Chemical Engineering Degree, with honors, in June 1947. At North Carolina State College he was a member of Lambda Chi Alpha social fraternity, and was made a member of the Tau Beta Pi, Phi Kappa Phi, Sigma Pi Alpha, and Gamma Sigma Epsilon honorary societies. During the summer of 1947, he attended the Université de Montréal where he received Le Certificat de Francais de la Section "A" avec la mention "grande distinction".

The following year he spent studying at the University of Wisconsin and was graduated in June 1948 with the degree of Master of Science in Chemical Engineering. The next year he studied at the Massachusetts Institute of Technology and received the Master of Science Degree in Chemical Engineering in September 1949. Dr. C. N. Satterfield was the advisor for his thesis, entitled "Some Explosive Characteristics of Hydrogen Peroxide Vapors."

In September 1949 he was made Research Engineer at the Engineering Experiment Station of the Georgia Institute of Technology, working with aerosols, and then liquid propellants. At the same time he entered the Graduate School of the Institute to complete the Ph.D. Degree in Chemical Engineering, minoring in physical chemistry. Also in 1949 he was made a Junior Member of the American Institute of Chemical Engineers.

On June 18, 1948 he was married to Ruth Heffner at the Chapel of the Cross in Chapel Hill, North Carolina. They have three children, Ruth Jeanne Eric, Robert Allen, Jr., and Kevin Crouse.